Bioorganic Chemistry 90 (2019) 103005

Contents lists available at ScienceDirect

Bioorganic Chemistry

journal homepage: www.elsevier.com/locate/bioorg

6-Substituted purines as ROCK inhibitors with anti-metastatic activity

Jiří Voller[a,b,*], Lenka Zahajská[c], Lucie Plíhalová[a,d], Jana Jeřábková[a], David Burget[a], Andreea Csilla Pataki[e], Vladimír Kryštof[a], Marek Zatloukal[d], Jan Brábek[e], Daniel Rösel[e], Václav Mik[d], Martin Tkáč[a], Tomáš Pospíšil[d], Tomáš Gucký[d], Karel Doležal[a,d], Miroslav Strnad[a]

[a] Laboratory of Growth Regulators, The Czech Academy of Sciences, Institute of Experimental Botany & Palacký University, Šlechtitelů 27, CZ-78371 Olomouc, Czech Republic

[b] Department of Clinical and Molecular Pathology, Institute of Molecular and Translational Medicine, Faculty of Medicine and Dentistry, Palacký University, Hněvotínská 3, 775 15 Olomouc, Czech Republic

[c] Isotope Laboratory, The Czech Academy of Sciences, Institute of Experimental Botany, Vídeňská 1083, 142 00 Prague 4, Czech Republic

[d] Department of Chemical Biology and Genetics, Centre of the Region Haná for Biotechnological and Agricultural Research, Palacký University, Šlechtitelů 27, CZ-78371 Olomouc, Czech Republic

[e] Department of Cell Biology, Faculty of Science, Charles University in Prague, Viničná 7, 12843, Prague 2, Czech Republic

ARTICLE INFO

Keyword:
Protein kinase inhibitor
ROCK
Anti-metastatic activity
Melanoma

ABSTRACT

Rho-associated serine/threonine kinases (ROCKs) are principal regulators of the actin cytoskeleton that regulate the contractility, shape, motility, and invasion of cells. We explored the relationships between structure and anti-ROCK2 activity in a group of purine derivatives substituted at the C6 atom by piperidin-1-yl or azepan-1-yl groups. Structure-activity relationship (SAR) analyses suggested that anti-ROCK activity is retained, and may be further increased, by substitution of the parent compounds at the C2 atom or by expansion of the C6 side chain. These inhibitors of ROCK can reach effective concentrations within cells, as demonstrated by a decrease in phosphorylation of the ROCK target MLC, and by inhibition of the ROCK-dependent invasion of melanoma cells in the collagen matrix. Our study may be useful for further optimization of C6-substituted purine inhibitors of ROCKs and of other sensitive kinases identified by the screening of a broad panel of protein kinases.

1. Introduction

Rho-associated serine/threonine kinases (ROCKs) are members of the AGC (cAMP-dependent protein kinase/protein kinase G/protein kinase C) protein kinase family. The human genome contains two ROCK genes: *ROCK1* and *ROCK2*. The isoforms share about 60% of amino acid sequences and about 90% homology in the kinase domain. The amino acids in the ATP binding sites of both isoforms are identical, making design of selective inhibitors difficult (reviewed in [7]).

ROCKs are principal regulators of the actin cytoskeleton. Through changes to actomyosin, ROCKs regulate cell contractility, cell shape, cell motility, cell invasiveness, and other cell functions. They also play an important role in the regulation of cellular metabolism, growth, division, and apoptosis. ROCKs also modulate neurite outgrowth, cell-cell adhesion, and angiogenesis (for a recent review see [23]).

ROCKs are activated by the small GTPase RhoA and phosphorylate various substrates, including myosin light chain phosphatase (MLCP). MLCP subsequently dephosphorylates the myosin light chain (MLC), resulting in the contraction of the actin cytoskeleton. ROCKs can also phosphorylate MLC directly. Other ROCK substrates involved in the regulation of the actin filament states are LIM kinases 1 and 2, adducin, and ezrin-radixin-moesin (for a review see [25]).

Both ROCK isoforms are expressed ubiquitously in mice. However, the levels of expression of the two isoforms differ in some tissues [30]. Intracellular distribution of ROCK isoforms is cell-type dependent and can differ between ROCK1 and ROCK2 [13]. Knockout mice for each ROCK isoform demonstrated that the isoforms cannot fully compensate for each other. In some contexts, they may even play opposing roles [13].

Both ROCK isoforms are mutated in cancers. The constitutively-active ROCK1 was found in breast and lung carcinomas [10,22]. Polymorphism in ROCK1 was also associated with the development and progression of prostate cancer [20]. ROCK2 mutations were observed in gastric cancer and melanoma (see review by [48]). Some mutations are located in the homologous sequences of both isoforms. Increased ROCK expression and/or activity has been correlated with tumour

* Corresponding author at: Laboratory of Growth Regulators, The Czech Academy of Sciences, Institute of Experimental Botany & Palacký University, Šlechtitelů 27, CZ-78371 Olomouc, Czech Republic.
E-mail address: jiri.voller@upol.cz (J. Voller).

https://doi.org/10.1016/j.bioorg.2019.103005
Received 31 December 2018; Received in revised form 31 March 2019; Accepted 19 May 2019
Available online 06 June 2019

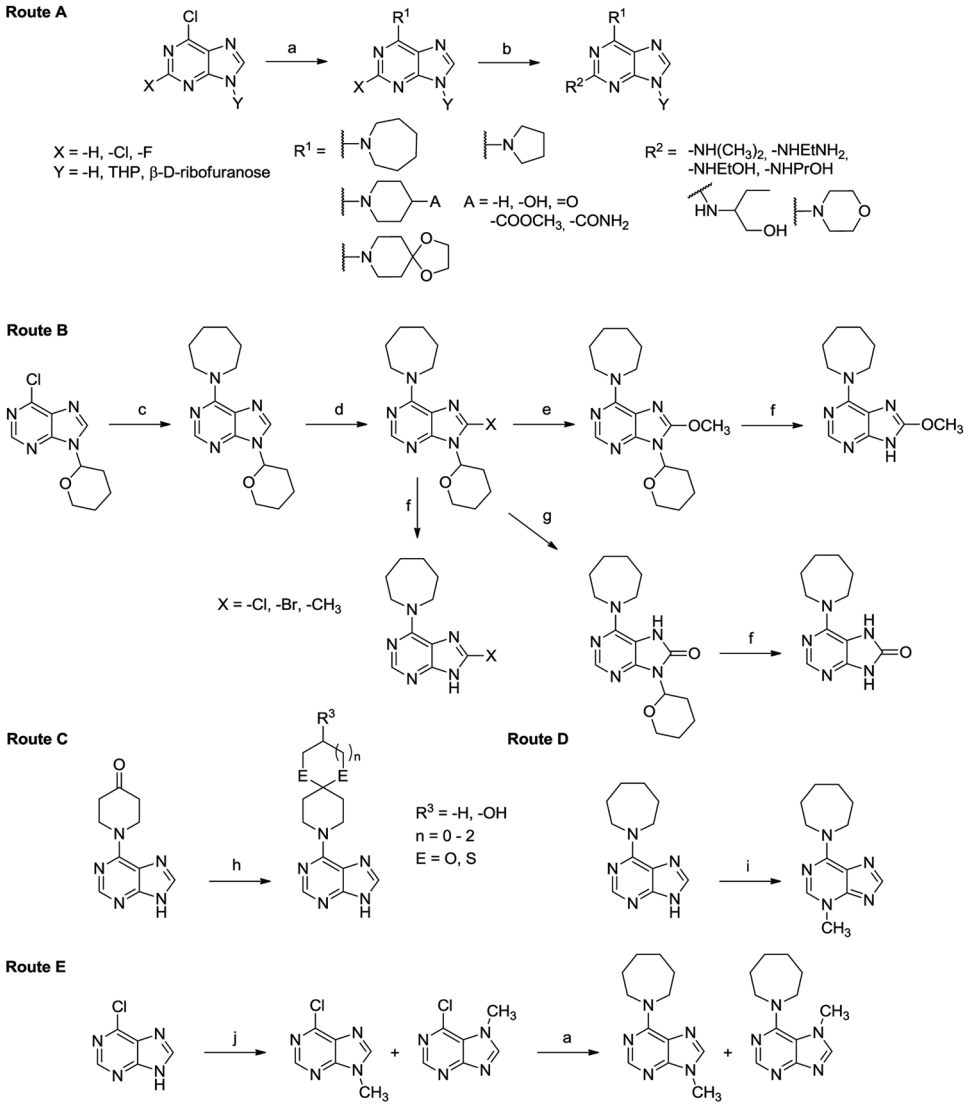

Fig. 1. Outlines of the syntheses. a) R^1-H, TEA, PrOH/*i*PrOH/DMF, rt - reflux; b) R^2-H, 165 °C, 115 °C for **8** and **9**; c) azepane, TEA, 2-propanol, 45 °C; d) 1. LDA, 2. $C_2Cl_6/CBr_4/CH_3I$, THF, −78 °C, 1 + 1 h; e) Na, CH_3OH, 60 °C, 32 h; f) 10% HCl, CH_3OH, 60 °C; g) Na, BnOH, 90 °C, overnight; h) diol/mercaptoethanol/1,2-ethanedithiol/glycerol, toluene, *p*-TsOH, 104 °C; i) MeI, DMA, 80 °C; j) MeI, K_2CO_3, DMF, rt.

aggressiveness [18,49,21].

The actin cytoskeleton functions in a range of processes that contribute to the development and progression of malignancies: cell adhesion, migration, and invasion; epithelial-mesenchymal transition; metastasis; neoangiogenesis; and immune cell infiltration [27]. Moreover, reorganization of the actin cytoskeleton modulates gene expression, cell cycle progression, vesicular transport, and extracellular matrix metabolism [35,12].

The Rho-ROCK pathway regulates tumour invasion and metastasis. Its association with distant metastases has been observed in breast [45], ovarian [4], gastric [24], and liver cancers [11]. Tumour cells invade either by amoeboid or mesenchymal movement depending on the extracellular matrix proteolysis. A change in motility mode is accompanied by cell morphology change – mesenchymal cells are protracted and amoeboid cells are spherical. The Rho-ROCK pathway regulates the ameboid migration [31]. However its role in the mesenchymal movement appears to be limited.

The anti-angiogenic and anti-metastatic activities of ROCK inhibition have been demonstrated in vitro on numerous occasions (see review by [36]). The administration of ROCK inhibitors fasudil, Y-27632, Wf-536, RKI-1447, and several other inhibitors reduced the growth of breast, hepatocellular or lung carcinomas, myeloma, and neuroblastoma in xenograft experiments [14,44,28,50,33,6]. Invasiveness and dissemination were reduced by these inhibitors in melanoma, fibrosarcoma, and carcinomas of breast, kidney, liver, and prostate (review by [7]).

In vitro and *in vivo* experiments suggest that ROCK inhibitors may be useful for treating a variety of other pathological conditions, including glaucoma, hypertension, asthma, erectile dysfunction, neurodegeneration, kidney failure, and osteoporosis. Since identification of their therapeutic potential, ROCK inhibitors with a wide variety of scaffolds have been reported [8,47,5]. Until now, only a few examples of ROCK2-selective compounds have been described (WO2015054317; [42]).

Many ROCK inhibitors also show only limited selectivity toward other kinases, especially other members of the AGC family. This is also true for the isoquinoline fasudil and the pyridine carboxamide Y-27632, the two “classical” ROCK inhibitors most widely used in *in vitro* and animal studies. Fasudil and related ripasudil have been approved in Japan for treating cerebral vasospasm during subarachnoid haemorrhage and glaucoma, respectively. Netarsudil, another isoquinoline derivative was approved for glaucoma treatment by FDA in 2017.

Table 1

The structures of the prepared compounds and their IC_{50} values for ROCK2.

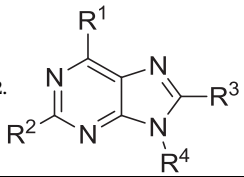

Compound number	R1	R2	R3	R4	IC_{50} [μM]
1	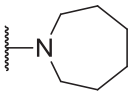	H	H	H	5.7 (± 1.6)
2		F	H	H	64.2 (± 4.6)
3		Cl	H	H	> 100
4		2-aminoethylamino	H	H	14.4 (± 1.5)
5		2-hydropropylamino	H	H	4.5 (± 0.8)
6		3-hydroxypropylamino	H	H	2.9 (± 0.6)
7		(1-hydroxybutan-2-yl)amino	H	H	5.3 (± 1.3)
8		dimethylamino	H	H	> 100
9		morpholino	H	H	> 100
10		H	Cl	H	> 100
11		H	Br	H	> 100
12		H	$-CH_3$	H	> 100
14		H	$-OCH_3$	H	> 100
15		H	H	$-CH_3$	> 100
16		H	H	THP	> 100
17		H	H	β-D-Rb	> 100
18		H	Cl	THP	> 100
19		H	Br	THP	> 100
20		H	$-CH_3$	THP	> 100
22	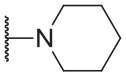	H	H	H	7.6 (± 1.0)
23		H	H	THP	> 100
24		H	H	β-D-Rb	> 100
25	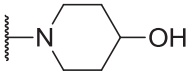	H	H	H	11.0 (± 1.4)
26	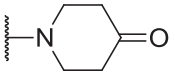	H	H	H	15.6 (± 4.1)
27		Cl	H	H	> 100
28		H	H	THP	> 100
29	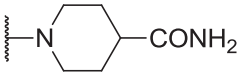	H	H	H	7.9 (± 1.9)
30	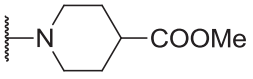	H	H	H	12.2 (± 2.6)
31	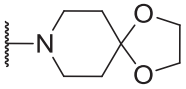	H	H	H	8.5 (± 0.5)
32		2-hydroxyethylamino	H	H	18.9 (± 3.5)
33		Cl	H	H	> 100
34		H	H	THP	> 100
35	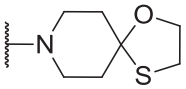	H	H	H	4.7 (± 1.2)
36	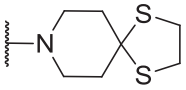	H	H	H	2.6 (± 1.0)
37		Cl	H	H	> 100
38		2-hydroxyethylamino	H	H	1.5 (± 0.4)
39	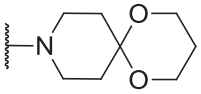	H	H	H	12.5 (± 1.6)
40	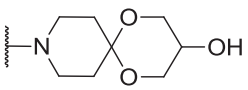	H	H	H	9.9 (± 1.5)
41	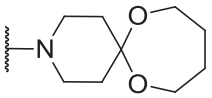	H	H	H	6.8 (± 1.1)

(*continued on next page*)

Table 1 (*continued*)

Compound number	R1	R2	R3	R4	IC_{50} [μM]
44	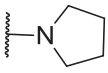	H	H	H	10.1 (± 2.1)
45		Cl	H	H	> 100
46		2-hydroxyethylamino	H	H	25.1 (± 4.6)
47		3-hydroxypropylamino	H	H	36.7 (± 3.1)

13: 6-(azepan-1-yl)-7,9-dihydro-8*H*-purin-8-one (IC_{50} > 100 μM). 21: 6-(azepan-1-yl)-9-(tetrahydropyran-2-yl)-7,9-dihydro-8*H*-purin-8-one (IC_{50} > 100 μM). 42: 6-(azepan-1-yl)-3-methylpurine (IC_{50} > 100 μM). 43: 6-(azepan-1-yl)-7-methylpurine (IC_{50} > 100 μM). THP: tetrahydropyran-2-yl; Rb: ribofuranosyl. IC_{50} values are given as mean ± standard deviation.

In this study we explored the relationship between the structure of purine derivatives substituted at the C6 atom by the piperidin-1-yl group or the azepan-1-yl group and ROCK2 inhibitory activity. We started with parent compounds (**1**, **22**) that have been identified as micromolar ROCK2 inhibitors in a high-throughput screening campaign (Pubchem AID:644). The screening set included also several less active derivatives with a substitution on the piperidine ring (**25**, **26**, **29**, **31**). Yet, to our knowledge, no follow-up studies (structure optimization, cell-based experiments) of these compounds have been conducted.

In the C6-azepanyl series, we evaluated the effects of substitutions in the C2, *N*3, *N*7, C8, and *N*9 positions of the purine moiety on anti-ROCK2 activity. In the series of C6-piperidinyl derivatives, substitutions at position 4 of the piperidine ring were studied. The piperidinyl derivatives included various spirocycles resulting from the reactions of the 4-oxopiperidine moiety with small diols and dithiols. We also explored anti-ROCK2 activity of several C6-pyrrolidin-1-yl derivatives with the substitutions that were promissing in the other series.

Furthermore, we studied the effects of new inhibitors on phosphorylation of downstream effector MLC2, as well as their influence on cellular morphology and invasiveness in a 3D collagen matrix using human melanoma (A2058 and A375m2) and fibrosarcoma (HT1080) cell lines as representatives of amoeboid or mesenchymal phenotypes, respectively.

2. Results

2.1. Synthesis

The straightforward syntheses of 6-monosubstituted and 2,6-disubstituted purines (Fig. 1, Route A) were carried out by the conventional method (see [2]). Commercially available 6-chloropurine or 2,6-dichloropurine were heated with azepane, pyrrolidine, piperidine, or piperidine derivatives preferably in *n*-propanol or 2-propanol in the presence of triethylamine. Well-known differences in the reactivity of 6-chloropurine, 2,6-dichloropurine, and 2-chloro-6-substituted purines towards nucleophilic substitution [26,3] were reflected in the times and temperatures needed for completion of reactions. Whereas 2,6-dichloropurine converted into 6-substituted product within 1.5–2 h at 65 °C (**3**, **27**, **33** and **45**), 6-chloropurine underwent substitution over 20 h at 90 °C (**1**, **22**, **25**, **26**, **29–31**). The subsequent substitution of the chlorine atom in 2-chloro-6-substituted purines requires harsher conditions. Thus, for the synthesis of compounds **4–9**, **32**, **38**, **46** and **47**, the solvent of choice was the used amine itself (in the case of dimethylamine it was its 50% solution in methanol). The reaction with secondary amines was usually completed by heating overnight at 90 °C, while reactions with primary amines required heating at 160 °C for durations ranging from 4 h to overnight.

The 8-substituted purines of the azepanyl series were prepared by four-step synthesis (Fig. 1, Route B). We selected 6-chloro-9-(tetrahydropyran-2-yl)purine as a starting material due to the ability of the THP group to enhance the reactivity of the chlorine in position 6 in the first step (**16**, **23**, **28**, **34**) as well as the reactivity of the halogen in position 8 in the third step of the synthesis. The THP group also serves as a protecting group in the second step of the procedure. Finally, it can be easily removed by acidic hydrolysis to produce free purine base in the last step of the synthesis (**10–14**). A halogen atom or methyl group was introduced into position 8 of 6-(azepan-1-yl)-9-(tetrahydropyran-2-yl)purine by lithiation and subsequent addition of a halogen donor or iodomethane (1. LDA in THF, −70 °C, argon atmosphere; 2. e.g. hexachloroethane, 1 h; **18–20**; [29]. The halogen atom in position 8 was subsequently substituted with benzyl alcoholate and methanolate to produce the 8-hydroxy derivative **21** and the 8-methoxy derivative **14** (after acidic hydrolysis of the THP group), respectively.

The presence of the keto group in **26** inspired us to synthesize derivatives with acetal-like spirocycles (**35**, **36**, **39–41**; Fig. 1, Route C). We employed conditions generally recommended for protection of carbonyl groups [16]. The reactions were carried out in toluene and catalysed by *p*-toluenesulfonic acid. Dehydration was accomplished by continuous azeotropic distillation. Acceptable product yields (60–83%; apart from **40** with a yield of 24%) were obtained despite the low solubility of the starting material in toluene.

2.2. Kinase assay with recombinant ROCK2 and analysis of structure-activity relationships (SARs)

Inhibition of ROCK2 was evaluated using a biochemical kinase test based on the measurement of the incorporation of radioactive phosphate from ATP into the oligopeptide substrate that is a part of the ROCK target sequence. The IC_{50} values of the parent compounds 6-(azepan-1-yl)purine (**1**) and 6-(piperidin-1-yl)purine (**22**) were 5.7 μM and 7.7 μM, respectively.

In the 6-azepanyl series (Table 1), any substitution in positions *N*9, *N*7, *N*3 and C8, including a methyl group (**15**, **43**, **42**, **12**) led to a loss of the ROCK2 kinase activity (IC_{50} > 100 μM). Other explored 8-substituents included hydroxy, methoxy, bromo and chloro functional groups (**13**, **14**, **11**, **10**). The group of inactive derivatives also included those with larger *N*9-substituents such as tetrahydropyran-2-yl (**16**) or β-D-ribofuranosyl (**17**). A similar loss of inhibitory activity against ROCK2 after *N*9-substitution of purine was also observed in the 6-piperidinyl series (**23**, **24**). The inactivity of the ribosides suggests that the mode of binding of the ROCK inhibitors we investigated differs from that of ATP. No inhibitory activity was observed among the 8,9-disubstituted purine derivatives (**18–21**).

On the other hand, several active derivatives were obtained after substitution of the purine C2 atom with hydroxyalkylamino groups. While an improvement in potency was observed for the 3-hydroxypropylamino derivative (**6**, IC_{50} = 2.9 μM), compounds substituted with the 2-hydroxyethylamino (**5**, IC_{50} = 4.5 μM) and (*R/S*)-1-hydroxymethylpropylamino (**7**, IC_{50} = 5.3 μM) groups demonstrated activity that was comparable to that of the parent compound. The 2-aminoethylamino derivative (**4**) was about three times less potent than the parent compound, and the C2 substitutions by chloro (**3**), fluoro (**2**), dimethylamino (**8**), and morpholin-4-yl (**9**) groups abolished the activity completely.

In the C6-piperidinyl series (Table 1 continued), the C4 substitution of piperidine with an aminocarbonyl group yielded the derivative (**29**) with activity (IC_{50} = 7.9 μM) comparable to that of the parent compound. The 4-hydroxyl (**25**), 4-methoxycarbonyl (**30**) and 4-oxo (**26**)

derivatives were less active, with IC_{50} values of 11.0 μM, 12.2 μM, and 15.6 μM, respectively. The reaction of the 4-oxo group with diols was used to synthesise ketals. The most active derivative was the one with the 7,12-dioxa-3-azaspiro[5.6]dodecane moiety at the C6 purine atom (**41**, IC_{50} 6.8 μM). Its activity was comparable to that of the unsubstituted 6-piperidin-1-yl-purine (**22**). The compounds prepared by reactions with shorter diols, like **31** (8.5 μM) and **39** (12.5 μM), and those including a glycerol derivative (**40**, 9.9 μM) were less active, but were more potent than 6-(4-oxopiperidin-1-yl)purine (**26**). We also prepared analogues of 6-(1,4-dioxa-8-azaspiro[4.5]decan-8-yl)purine (**31**) where one oxygen atom (**35**, IC_{50} = 4.7 μM) or both oxygen atoms (**36**, IC_{50} = 2.6 μM) were replaced by sulphur. Although 1,3-dithiolane and 1,3-oxathiolane moieties are unusual in drug design, examples of their successful use do exist – the ACE inhibitor spirapryl and anti-muscarinic agent cevimeline serve as examples. Like the 8-substituted compounds from the azepanyl series, the spirocycles were prepared by acid hydrolysis of the respective 9-tetrahydropyran-2-yl derivatives. None of those precursors demonstrated inhibitory activity in a ROCK2 assay.

Based on the SAR knowledge originating from the 6-azepanyl series, spirocyclic derivatives **36** and **31**, with a 2-hydroxyethylamino group at the purine C2 atom, were prepared by nucleophilic substitution of the respective 2-chloro derivatives (**33**, **37**; both IC_{50} > 100 μM) yielding compounds **38** (IC_{50} 1.5 μM) and **32** (IC_{50} 18.9 μM).

Finally, we also explored the effect of the substitutions of 6-(pyrrolidin-1-yl)purine (**44**, IC50 = 10.1 μM) at the purine C2 atom with selected hydroxyalkylamino sidechains that improved activity of 6-(azepan-1-yl)purine. However, both derivatives (**46**, **47** IC50 > 25 μM) were significantly less active than the parent compound. This observation suggests that a bulkier N^6-substituent is required for an efficient interaction with the binding site or ROCK2.

Overall our SAR study demonstrates that the parent ROCK inhibitors 6-(azepan-1-yl)purine (**1**) and 6-(piperidin-1-yl)purine (**22**) can be modified by a substitution at the purine C2 atom and by an expansion of the sidechain at the purine C6 atom. On the other hand, all the substitutions on the imidazole ring or *N*3 nitrogen of the purine moiety led to loss of inhibitory activity. Although some derivatives have improved IC_{50} values compared to the parent compounds, none was more potent than the classical ROCK inhibitors fasudil (IC_{50} = 1.1 μM) and Y-27632 (IC_{50} = 0.8 μM).

2.3. Evaluation of kinase selectivity of the selected compounds

A single concentration (50 μM) of the two most active disubstituted derivatives **6** and **38** were tested on a commercial panel (DiscoverX, USA) of 96 kinases (Supplemental Table S1). The assay uses a DNA-labelled kinase that is captured on a solid matrix derivatized with its substrate. When the test compound binds to the matrix, kinases are released into the solution and the kinase concentrations are quantified by PCR. Compound **6** released ≥99% of the bound ROCK2, JAK3, JNK1-3 (MAPK 8–10), RSK2, and SNARK. The list of kinases that are highly sensitive to the more hydrophobic **38** includes these same kinases, except for JNK2 and RSK1, as well as 9 additional kinases (ARK5, AXL, CSF1R, DYRK1B, ERK8, JAK2, MKNK, TYK2, and ULK2). Lower selectivity is also apparent for other cut-off levels, e.g. at 90%. Subsequently K_d values for **38** and ROCK2 (0.5 μM), ROCK1 (1.3 μM), JAK1 (> 25 μM), JAK2 (2.2 μM), and JAK3 (1.4 μM) were determined using the same assay. Kinase selection was based on Discoverx ScanEdge panel, but some kinases were replaced to enrich the panel for known off-target kinases of other ROCK inhibitors including fasudil, Y-27632, H-7/8, H-89, and H-1152. Interestingly, some of the kinases inhibited by all or most of those ROCK inhibitors were insensitive toward our compounds. For example, the residual activities for MKNK1 were 72% and 45% for **6** and **38**, respectively. PKAC-α (100% and 87%) and PKAC-β (98% and 62%) were even less sensitive.

2.4. Effect of the compounds on cell proliferation

A resazurin assay (3-day incubation) was used to evaluate the effect of the compounds on cell proliferation. IC_{50} values were calculated from dose-response curves. For human non-malignant cells (skin fibroblasts BJ, keratinocytes HaCaT, and retinal epithelial cells ARPE-19), IC_{50} values were always higher than 50 μM and no effect on proliferation was observed at 12.5 μM (data not shown). Inhibitor compounds **1**, **5**, **38**, and positive controls fasudil and Y-27632 were also tested on HT1080, A375m2, and A2058 melanoma cell lines. The IC_{50} values for **1** were 70.5 μM, 37.1 μM, and 26.8 μM respectively. All IC_{50} values for the other two compounds tested were above 100 μM, the highest concentration tested. For compounds **5** and **38**, no effects on proliferation were observed after application of 10 μM, the concentration used in the follow-up cell-based experiments. For **1**, the resazurin signal decrease was lower than 5%. Comparable small negative effects on cell proliferation were observed for both control compounds fasudil and Y-27632.

2.5. The effect of new ROCK inhibitors on downstream signalling

One downstream effect of ROCK on the actin cytoskeleton and traction forces of cells occurs via the phosphorylation of the myosin light chain (MLC; [15,19]). Therefore, we evaluated MLC2 phosphorylation after a 24-h treatment with ROCK inhibitors using Western blot. The intensities of MLC2 and pMLC2 (T18/S19) signals were measured by densitometry. Inhibitors **1**, **5,** and **38** at concentrations of 10 μM significantly decreased MLC2 phosphorylation in A375m2, A2058, and HT1080 cells (Figs. 2 and S1). Their effects were comparable to equimolar fasudil but, in the melanoma cells, their activity was markedly lower than that of Y-27632. These results show that the new purine inhibitors can reach relevant concentrations in the cells.

2.6. Treatments with new purine ROCK inhibitors alters cellular morphology in 3D collagen and reduces invasiveness of human melanoma cells

Classical ROCK inhibitors like Y-27632 are proven inhibitors of amoeboid movement of melanoma cells, and they change the morphology of these cells to a longer mesenchymal-type morphology [37,38]. Therefore, we tested newly prepared ROCK inhibitors at 10 μM concentrations for 3D morphology assays using A375m2 and A2058 melanoma cells. The HT1080 fibrosarcoma cell line served as a control. Equimolar concentrations of commercially available inhibitors fasudil and Y-27632 were compared. We observed that amoeboid melanoma cells mainly changed their morphology to the mesenchymal type upon treatment with either inhibitor (Fig. 3). Treatment of A375m2 cells with the prepared inhibitors **1**, **5**, and **38** increased the proportion of mesenchymal cells from less than 10% to 69.6–77.7%. The effects of fasudil and Y-27632 were slightly weaker (65.5% and 55.1%, respectively). In A2058 cells, the changes from the amoeboid to the mesenchymal phenotype after ROCK inhibition were also significant. While 93.9% of the vehicle-treated cells maintained their ameboid morphology, the treatment with the prepared inhibitors increased proportion of mesenchymal cells to 48.2–66.0%. For fasudil and Y-27632, the proportions of mesenchymal cells were 53.3% and 78.0%, respectively. As expected, the inhibitors had no effect on the morphology of the HT1080 cell line. These cells remained mainly mesenchymal (91–95%).

Since cell morphology is associated with invasion mode, we also tested the effects of both prepared and commercially available ROCK inhibitors (at 10 μM concentration) on the invasiveness of the cell lines. Treatment with either of the compounds significantly inhibited the invasiveness of melanoma cells into a rat collagen matrix. No significant effects were observed for the mesenchymal HT1080 cell line (Fig. 4).

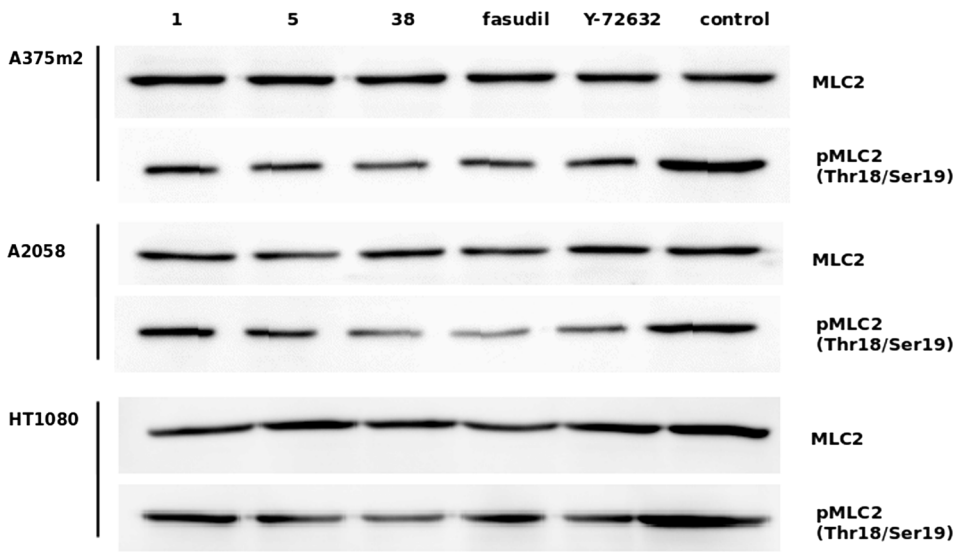

Fig. 2. Treatment with the prepared and established ROCK inhibitors decreases pMLC2(Thr18/Ser19)/MLC2 ratio.

3. Discussion

The Rho-associated serine/threonine kinases (ROCKs) are the principal regulators of the actin cytoskeleton. Through cytoskeleton changes, ROCKs regulate the growth, division, contractility, shape, motility, and death of cells. Pharmacological ROCK inhibitors may therefore be useful for treating a host of diseases where these cell processes are dysregulated including cancers.

Here we explored the ROCK2-inhibitory activity of a group of purine derivatives substituted at the C6 atom by the pyrrolidin-1-yl, piperidin-1-yl or azepan-1-yl group. A set of 47 compounds was prepared for this study, and the syntheses of 39 of these derivatives are described for the first time. Our SAR study suggests that ROCK2-inhibitory activity in piperidin-1-yl or azepan-1-yl series is retained and may even increase with substitution at the C2 purine atom on the parent compounds or with expansion of the side-chain at the C6 purine atom.

Kinase profiling of selected derivatives suggested that the 2,6-disubstituted purines we investigated may not possess selectivity for ROCK isoforms. However, some off-target kinases known to be inhibited by other ROCK inhibitors were insensitive to these select derivatives. These newly-developed purine derivatives may also serve as leads for the synthesis of inhibitors of JAK or JNK kinases. Development of dual-inhibitors of ROCK/JAK and/or ROCK/JNK may be also an interesting prospect. For example, Sanz-Moreno et al. [41] showed that ROCK and JAK1 signalling cooperate to control actomyosin contractility in tumour and stroma cells. Such dual inhibitory activity might be beneficial for treating illnesses, like fibrosis and inflammation, in which some of the processes regulated by ROCK, JNK and JAK1 contribute to the pathology. ROCK itself is known to regulate these processes (for a recent review, see [23]). A recent report suggested that combined ROCK/JAK/PDGFR-β inhibitors are active in models of choroidal neovascularization.

Since they regulate cytoskeletal functions, ROCKs play an important role in contractility, stress fibre formation, focal adhesion complex assembly, and in the cell migration and invasion that occurs during cancer metastasis [34,17]. The ROCK pathway is involved in both the main types of cancer cell migration: amoeboid and mesenchymal [39]; however, its role in amoeboid migration is critical. First-generation ROCK inhibitors like the commercially-available Y-27632 have demonstrated inhibition of the blebbing and highly contractile amoeboid movement and conversion of amoeboid melanoma cells into the more-elongated mesenchymal phenotype [39]. We observed similar effects in melanoma cell lines A375M2 and A2058 treated with either “classical” ROCK inhibitors or selected purine derivatives using the collagen matrix 3D cultures. Conversely, HT1080 fibrosarcoma cells exhibiting mesenchymal migration mode maintained their elongated morphology after the application of the inhibitors.

Since ROCK signalling is also involved in the invasiveness of melanoma cells [9,40,37,41,32,38], the selected derivatives were tested in a 3D collagen invasion assay. As expected, considering the previous study by Routhier et al. [37], Y-27632 inhibited the invasiveness of both amoeboid melanoma cell lines. Fasudil and the purine derivatives significantly suppressed invasion into the collagen as well. In contrast, the compounds were unable to suppress migration of mesenchymal HT1080 fibrosarcoma cells. Overall the observed effects of the compounds on the morphology and invasiveness of the amoeboid melanoma cell lines, and not mesenchymal fibroblastoma cell lines, agree with the presumed ROCK inhibition.

ROCKs modulate the actin cytoskeleton through phosphorylation of MLC, cofilin, and LIM kinases [1,46]. We studied the phosphorylation levels of MLC2 after treatment with the prepared compounds in all three cell lines to further confirm that the phenotypes observed resulted from ROCK inhibition. A significant decrease of pMLC was observed, as expected.

We synthesized a set of C6-substituted purines with ROCK-inhibitory activity for this SAR study. The study suggests that the active compounds can be obtained by select substitutions on the pyrimidine ring, while changes on the imidazole ring of the purine moiety are not tolerated. The inhibitors can reach effective concentrations within cells, as demonstrated either by decreased phosphorylation of the ROCK downstream target MLC, or by inhibition of the ROCK-dependent invasion of melanoma cells into the collagen matrix. These effects were observed at concentrations having no or marginal effects on cell proliferation. Our study may help researchers interested in further development of purines, and possibly their bioisosteres as well, into more potent ROCK inhibitors. The findings of our study could also inspire development of inhibitors of other kinases identified as sensitive by the kinase panel screening, like members of the JAK and JNK families.

4. Materials and methods

4.1. Chemistry

The chemicals, solvents for synthesis, and spectral solvents were purchased in analytical or HPLC grade quality from available suppliers

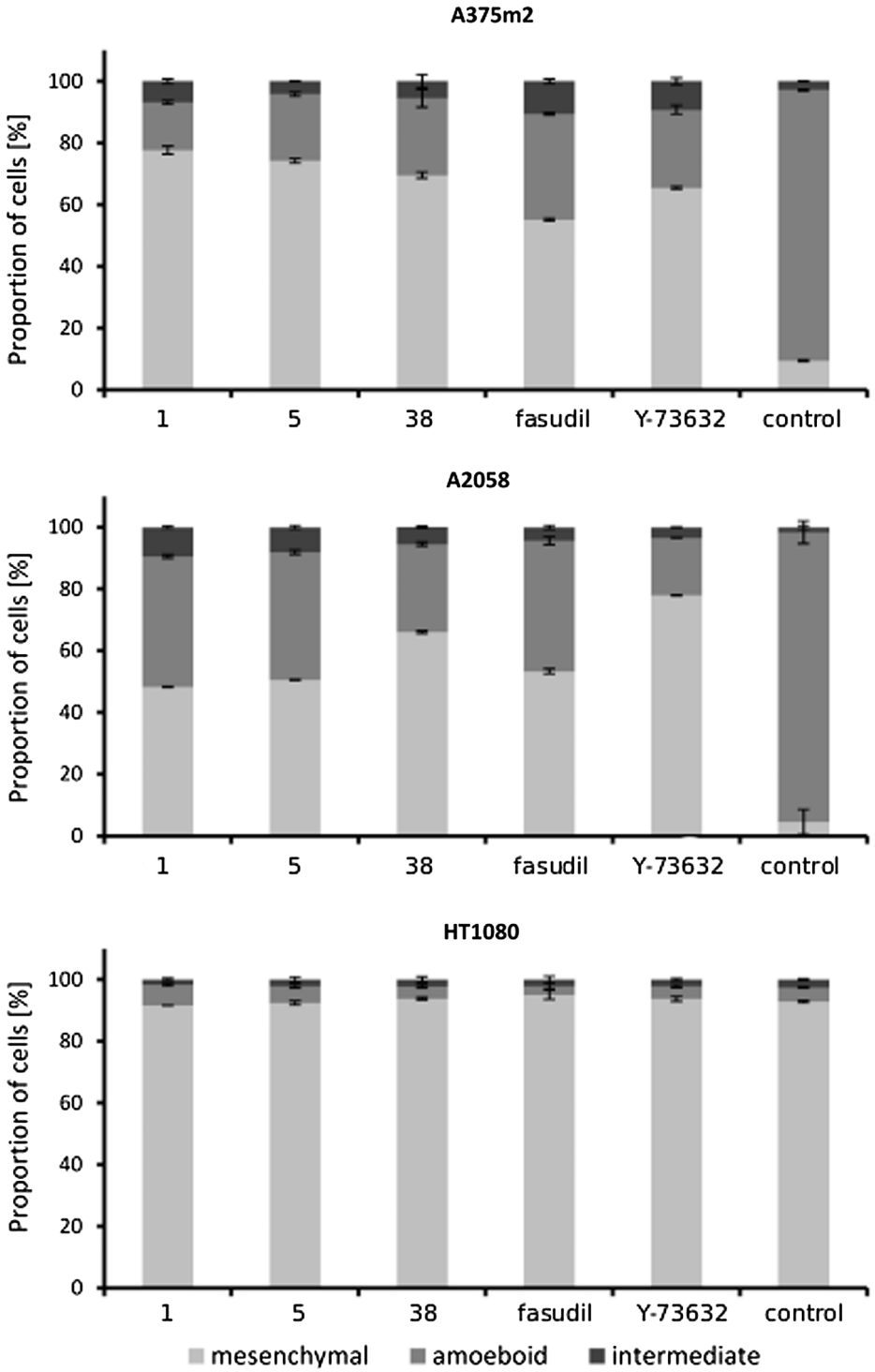

Fig. 3. Treatment with the prepared and established ROCK inhibitors induces morphology changes in melanoma cell lines A375m2 and A2058 but not in fibrosarcoma cell line HT1080.

and used without further purification. Microwave synthesis was performed in microwave reactor Discover SP (CEM Corporation) in 10 mL closed vessels using following set up: temperature 120 °C, power 150 W, ramp time 2 min, hold time 10 min, powermax on. Thin layer chromatography (TLC) was carried out using silica gel 60 F254 plates (Merck Co.). $CHCl_3$:MeOH:NH_4OH 95:5:0.5, 9:1:0.1, 8:2:0.2 or 7:3:0.3; $CHCl_3$:acetone 4:1 or 3:2 were used as mobile phases. Crude products were purified either by column chromatography using Silikagel 40–63 (VWR) or by middle pressure column chromatography (MP CC) using silica gel PharmPrep 60 CC (40–63 μm; Merck) as the stationary phase in a glass column (Kronlab, 15 mm diameter column or Pharmacia Fine Chemicals, 25 mm diameter column). As the mobile phase for MP CC, hexanes:EtOAc 3:2 or $CHCl_3$:MeOH:NH_4OH 95:5:0.5, 9:1:0.1 or 75:25:2.5 were applied. A flow rate of the mobile phase through the system was 7.5 mL/min. The purity of prepared compounds was confirmed by HPLC. Samples for HPLC (carried on a Beckman Gold system) were dissolved in MeOH, applied to a LiChroCARD 250 × 4 mm column filled with Purospher RP-18e, 5 μm (Merck) and the separated constituents were eluted by isocratic elution using a mixture of MeOH (HPLC grade) and AcOH/$AcONH_4$ buffer (pH 3.4; 40 mM; with addition

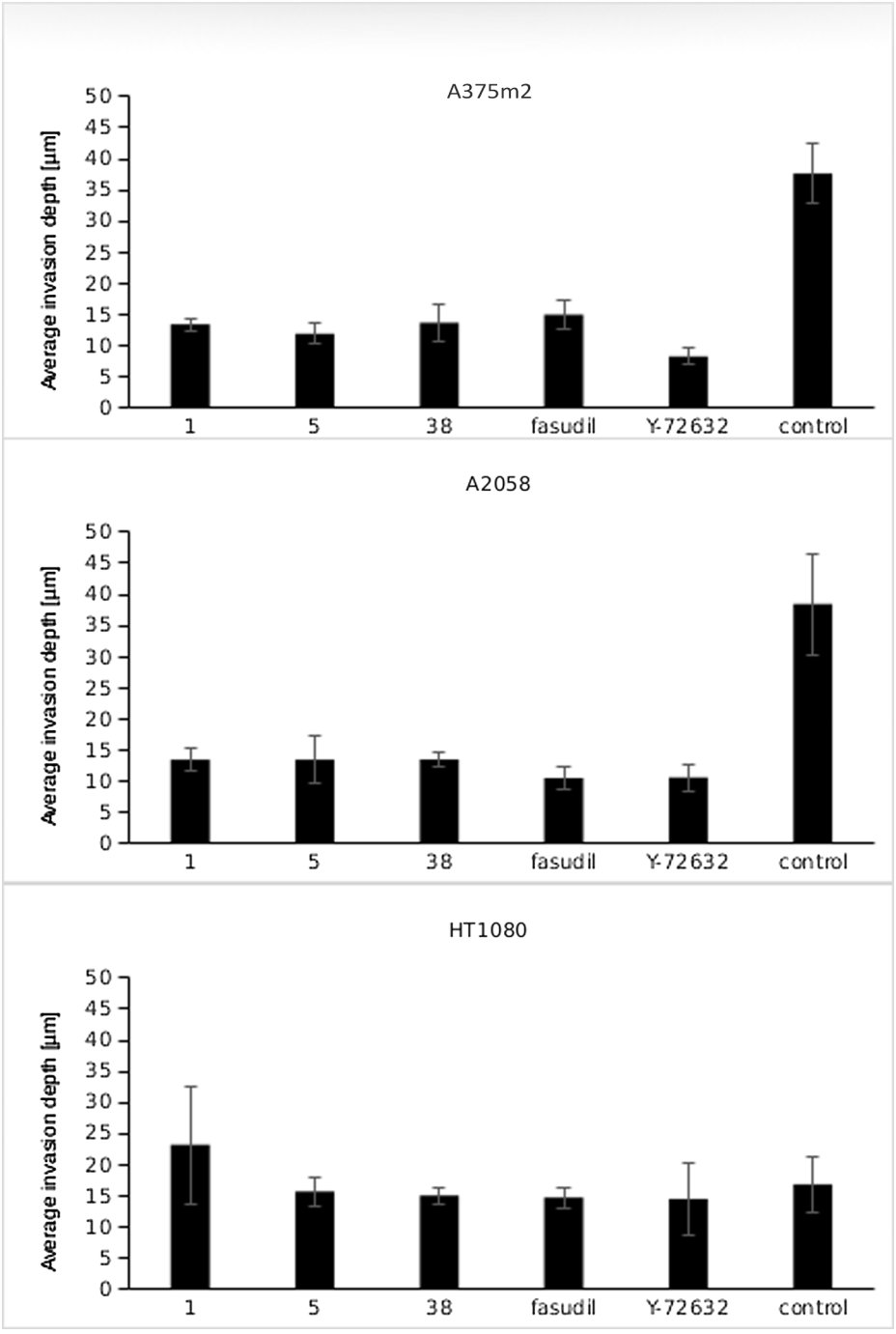

Fig. 4. Treatment with the prepared and established ROCK inhibitors inhibits invasion of melanoma cell lines A375m2 and A2058 into collagen 3D matrix.

of 5% MeOH) at a flow rate of 0.5 mL/min. The mixture contained 50%, 60%, 70% or 80% MeOH. Eluting compounds were detected by scanning the UV absorbance of the eluate between 200 and 300 nm. Elemental analyses were performed using a CHN-O analyser, Thermo Finnigan Flash, EA 1112 series; the values (C, H, N) agreed with the calculated ones within acceptable limits. Mass spectra were measured on a MS Waters/Micromass, ZMD-detector, direct inlet, ESI coin voltage 20 V. ^{1}H NMR spectra were recorded on a Bruker Avance 300 spectrometer operating at 300 K and frequency of 300 MHz (^{1}H), 75 MHz (^{13}C) or a JEOL ECA-500 spectrometer operating at 298 K and frequency of 500 MHz (^{1}H) and 125 MHz (^{13}C). Samples were dissolved in DMSO-d_6, $CDCl_3$ or CD_3OD. The NMR spectra were calibrated on residual solvent peak: DMSO-d_6 (^{1}H 2.49 ppm, ^{13}C 39.52 ppm), $CDCl_3$ (^{1}H 7.26 ppm, ^{13}C 77.0 ppm), CD_3OD (^{1}H 3.31 ppm, ^{13}C 49.0 ppm). The note (cv) in the text means that the signal was partly covered by another signal.

4.1.1. 6-(Azepan-1-yl)purine (1)

6-Chloropurine (2 g, 12.9 mmol) was refluxed with azepane (14.8 mL, 131.1 mmol) at 80–90 °C for 3 h. The reaction was monitored via TLC ($CHCl_3$:MeOH 4:1), concentrated *in vacuo*. The residue was dissolved in EtOAc and mixed with distilled H_2O. The layers were separated. The EtOAc layer was dried over Na_2SO_4, filtered, and evaporated *in vacuo*. Crude product was air-dried. White solid. Yield: 2.56 g (91%). M.p.: 285–290 °C dec. HPLC R_t = 10.3 min (70% MeOH + 30% buffer); UV (80% MeOH + 20% buffer) λ_{min} 235 nm, λ_{max} 279 nm;

HPLC purity > 99%. MS ESI+ (CV 17) *m/z* (rel. %): 218.4 (100) $[M+H]^+$, 240 (27) $[M+Na]^+$, 435 (47) $[2M+H]^+$. ^{1}H NMR (500 MHz, DMSO-d_6) δ (ppm): 1.48 (bs, 4H, azep), 1.76 (bs, 4H, azep), 3.82 (bs, 2H, azep), 4.33 (bs, 2H, azep), 8.06 (s, 1H, pur H8), 8.15 (s, 1H, pur H2), 12.90 (bs, 1H, pur NH). ^{13}C NMR (125 MHz, DMSO-d_6) δ (ppm): 26.3, 26.7, 28.7, 47.5, 49.0, 118.4, 137.9, 151.1, 151.9, 153.5.

4.1.2. 6-(Azepan-1-yl)-2-fluoropurine (2)

6-Chloro-2-fluoro-9*H*-purine (172 mg, 1 mmol), azepane (113 µL, 1 mmol), and triethylamine (420 µL, 3 mmol) were refluxed in PrOH at 95–98 °C while stirring for 4 h. The reaction mixture was then cooled down to room temperature and evaporated to give a yellow solid residue which was treated with water (20 mL). The precipitated yellow solid was filtered off, washed with water, and dried. The crude product was crystallized from methanol (10 mL). White powder. Yield: 80 mg (34%). HPLC purity > 99%. ESI+ (CV 20) *m/z* (rel. %): 236 $[M+H]^+$ (100). ^{1}H NMR (500 MHz, DMSO-d_6) δ (ppm): 1.50 (bs, 4H, azep), 1.77 (bs, 4H, azep), 3.76 (bs, 2H, azep), 4.35 (bs, 2H, azep), 8.06 (s, 1H, pur H8), 13.06 (bs, 1H, pur NH). ^{13}C NMR (125 MHz, DMSO-d_6) δ (ppm): 26.1, 26.2, 26.4, 28.5, 47.9, 49.0, 116.8, 138.5, 152.5 (d, J = 20.5 Hz), 154.6 (d, J = 20.5 Hz), 158.2 (d, J = 201.0 Hz). Anal.: Calcd. for $C_{11}H_{14}FN_5$, M_r = 235.27: C 56.16; H 6.00; N 29.77%. Found: C 56.33; H 5.98; N 29.38%.

4.1.3. 6-(Azepan-1-yl)-2-chloropurine (3)

2,6-Dichloropurine (2 g, 10.6 mmol) was refluxed with azepane (1.4 mL, 11.6 mmol) and Et_3N (5.9 mL, 42.3 mmol) in PrOH (40 mL) at 100 °C for 4 h. The reaction mixture was then cooled to room temperature and a solid was isolated. The solid was filtered off, washed with cold PrOH and cold H_2O, and dried at 50 °C. White powder. Yield: 2.1 g (78%). M.p.: 248–249 °C. HPLC R_t = 15.4 min (80% MeOH + 20% buffer); UV (80% MeOH + 20% buffer) λ_{min} 239 nm, λ_{max} 280 nm; HPLC purity 100%. MS ESI+ (CV 30) *m/z* (rel. %): 252 (100) $[M+H]^+$, 254 (33) $[M+H]^+$. ^{1}H NMR (300 MHz, DMSO-d_6) δ (ppm): 1.45 (bs, 4H, azep), 1.73 (bs, 4H, azep), 3.73 (bs, 2H, azep), 4.29 (bs, 2H, azep), 8.06 (s, 1H, pur H8), 13.07 (bs, 1H, pur NH).

4.1.4. 2-(2-Aminoethylamino)-6-(azepan-1-yl)purine (4)

6-(Azepan-1-yl)-2-chloropurine (**3**; 0.5 g, 2.0 mmol) was placed into a pressure tube with ethylenediamine (5.0 mL, 74.3 mmol) at 165 °C for 3 h. The mixture was then cooled to room temperature and concentrated *in vacuo*. The arisen precipitate was dissolved in cold H_2O and recrystallized. White powder. Yield: 0.5 g (96%). M.p.: 177–179 °C. ^{1}H NMR (500 MHz, DMSO-d_6) δ (ppm): 1.47 (bs, 4H, azep), 1.73 (bs, 4H, azep), 2.66 (t, J = 6.4 Hz, 2H, H_2N-C<u>H_2</u>-), 3.20 (q, J = 6.2 Hz, 2H, -C<u>H_2</u>-NH-), 3.75 (bs, 2H, azep), 4.24 (bs, 2H, azep), 6.10 (bs, 1H, -$(CH_2)_2$-N<u>H</u>-), 7.62 (s, 1H, pur H8). ^{13}C NMR (125 MHz, DMSO-d_6) δ (ppm): 26.3, 27.0, 29.0, 40.4, 41.3, 41.5, 44.3, 47.2, 48.6, 112.9, 134.5, 153.4, 153.6, 157.9, 158.8, 159.0.

4.1.5. 6-(Azepan-1-yl)-2-(2-hydroxyethylamino)purine (5)

6-(Azepan-1-yl)-2-chloropurine (**3**; 0.5 g, 2.0 mmol) reacted with ethanolamine (4.5 mL, 74.3 mmol) in a pressure tube at 165 °C for 3 h. Reaction mixture was cooled to room temperature which produced the precipitate. The precipitate was isolated and recrystallized in H_2O. Yield: 326.4 mg (56%). M.p.: 212 °C. ^{1}H NMR (500 MHz, DMSO-d_6) δ (ppm): 1.46 (bs, 4H, azep), 1.73 (bs, 4H, azep), 3.29 (q, J = 6.2 Hz, 2H, -NH-C<u>H_2</u>-), 3.49 (t, J = 6.2 Hz, 2H, -C<u>H_2</u>-OH), 3.74 (bs, 2H, azep), 4.24 (bs, 2H, azep), 4.66 (bs, 1H, -OH), 5.99 (t, J = 5.7 Hz, 1H, -CH_2-N<u>H</u>-), 7.63 (s, 1H, pur H8), 12.14 (bs, 1H, pur NH). ^{13}C NMR (125 MHz, DMSO-d_6) δ (ppm): 26.4, 27.0, 29.1, 44.0, 47.4, 48.7, 60.5, 113.0, 134.6, 153.3, 153.7, 158.9.

4.1.6. 6-(Azepan-1-yl)-2-(3-hydroxypropylamino)purine (6)

6-(Azepan-1-yl)-2-chloropurine (**3**; 217 mg, 0.86 mmol) was dissolved in 3-aminopropan-1-ol (2 mL). The solution was heated at 115 °C for 26 h and at 160 °C for 4 h. After cooling, the mixture was refrigerated for 2 weeks. The product crystallized from the mixture in lumps. Crystals (first portion) were filtered off, crushed on sintered glass, and washed thoroughly with H_2O (15 mL). The second portion of product was obtained from the filtrate which was diluted with H_2O while washing the crystals and then refrigerated for 1 d. The overall yield after drying both portions of product in a desiccator with P_2O_5 was 225 mg (90%). The raw product was crystallized from EtOH (20 mL). White wadding substance. Yield: 153 mg (61%). M.p.: 226–230 °C (>200 °C subl.). HPLC R_t = 5.1 min (75% MeOH + 25% buffer), R_t = 6.4 min (60% MeOH + 40% buffer); UV (75% MeOH + 25% buffer) λ_{max} 239 nm, λ_{min} 251 nm, λ_{max} 259 nm, λ_{min} 275 nm, λ_{max} 290 nm, HPLC purity > 99%. MS ESI+ (CV 18) *m/z* (rel. %): 291 $[M+H]^+$ (100); ESI$^-$ (CV 22) *m/z* (rel. %): 289 $[M]^-$ (100). ^{1}H NMR (500 MHz, DMSO-d_6) δ (ppm): 1.47 (bs, 4H, azep H4′, 5′), 1.65 (pent, J = 6.4 Hz, 2H, -CH_2-C<u>H_2</u>-CH_2-), 1.73 (bs, 4H, azep H3′, 6′), 3.25 (q, J = 6.5 Hz, 2H, -HN-C<u>H_2</u>-), 3.44 (t, J = 5.7 Hz, 2H, HO-C<u>H_2</u>-), 3.75 (bs, 2H, azep H2′), 4.24 (bs, 2H, azep H7′), 4.48 (bs, 1H, -OH), 6.07 (t, J = 5.8 Hz, 1H, -N^2-H), 7.61 (s, 1H, pur H8), 12.14 (bs, 1H, pur NH). ^{13}C NMR (125 MHz, DMSO-d_6) δ (ppm): 26.3 (azep C4′, 5′), 26.9 (azep C3′), 29.0 (azep C6′), 32.7 (-CH_2-<u>C</u>H_2-CH_2-), 38.3 (-HN-<u>C</u>H_2-), 47.3 (azep C2′), 48.7 (azep C7′), 58.9 (HO-CH_2-), 112.8 (pur C5), 134.4 (pur C8), 153.3 (pur C4), 153.6 (pur C6), 159.0 (pur C2).

4.1.7. 6-(Azepan-1-yl)-2-(1-hydroxymethylprop-1-ylamino)purine (7)

6-(Azepan-1-yl)-2-chloropurine (**3**; 216 mg, 0.86 mmol) was dissolved in 2-aminobutan-1-ol (2 mL). The solution was heated at 115 °C for 20 h and at 160 °C for 19 h. After cooling, the product was precipitated from the reaction mixture with H_2O (40 mL). The suspension was refrigerated overnight. The product crystallized from the mixture as a plaster-like substance. The milk-like precipitate was filtered off, washed thoroughly with H_2O (20 mL), and dried in a desiccator with P_2O_5. White plaster-like substance. Yield: 251 mg (96%). M.p.: 185–188 °C. HPLC R_t = 7.8 min (65% MeOH + 35% buffer); UV (65% MeOH + 35% buffer) λ_{max} 240 nm, λ_{min} 250 nm, λ_{max} 261 nm, λ_{min} 276 nm, λ_{max} 290 nm; HPLC purity 98%. MS ESI+ (CV 18) *m/z* (rel. %): 305 $[M+H]^+$ (100); ESI$^-$ (CV 23) *m/z* (rel. %): 303 $[M]^-$ (100). ^{1}H NMR (500 MHz, DMSO-d_6) δ (ppm): 0.86 (t, J = 7.3 Hz, 3H, -CH_3), 1.43 (quint (cv), J = 7.3 Hz, 1H, CH_3-C<u>H_2</u>-), 1.46 (bs (cv), 4H, azep H4′, 5′), 1.57 (quint, J = 6.8 Hz, 1H, CH_3-C<u>H_2</u>-), 1.73 (bs, 4H, azep H3′, 6′), 3.36 (bs, 1H, HO-C<u>H_2</u>- overlap with H_2O), 3.44–3.47 (m, 1H, HO-C<u>H_2</u>-), 3.74 (bs (cv), 3H, -HN-C<u>H</u> < and azep H2′), 4.24 (bs, 2H, azep H7′), 4.57 (bs, 1H, HO-), 5.63 (d, J = 8.5 Hz, 1H, -N^2-H), 7.61 (s, 1H, pur H8), 12.04 (bs, 1H, pur NH). ^{13}C NMR (125 MHz, DMSO-d_6) δ (ppm): 10.7 (-CH_3), 23.9 (CH_3-<u>C</u>H_2-), 26.4 (azep C4′, 5′), 26.9 (azep C3′), 29.0 (azep C6′), 47.2 (azep C2′), 48.6 (azep C7′), 54.0 (-HN-<u>C</u>H <), 63.1 (HO-CH_2-), 112.9 (pur C5), 134.5 (pur C8), 153.3 (pur C4), 153.6 (pur C6), 158.8 (pur C2).

4.1.8. 6-(Azepan-1-yl)-2-dimethylaminopurine (8)

6-(Azepan-1-yl)-2-chloropurine (**3**; 210 mg, 0.83 mmol) was dissolved in 50% solution of dimethylamine and MeOH (3 mL). The solution was heated at 60 °C for 16 h and at 115 °C for 4 h. After cooling, the mixture was refrigerated for 3 h. The product crystallized from the mixture as needles. Crystals were filtered off, washed thoroughly with MeOH (13 mL) and H_2O (30 mL), and dried in a desiccator with P_2O_5 for 2 d. White crystals. Yield: 113 mg (52%). M.p.: 237–238 °C (>200 °C subl.). HPLC R_t = 11.2 min (80% MeOH + 20% buffer); UV (80% MeOH + 20% buffer) λ_{max} 245 nm, $\lambda_{shoulder}$ 257–264 nm, λ_{min} 277 nm, λ_{max} 291 nm; HPLC purity > 99%. MS ESI+ (CV 17) *m/z* (rel. %): 261 $[M+H]^+$ (100), ESI$^-$ (CV 23) *m/z* (rel. %): 259 $[M]^-$ (100). ^{1}H NMR (500 MHz, DMSO-d_6) δ (ppm): 1.46 (bs, 4H, azep H4′, 5′), 1.75 (bs, 4H, azep H3′, 6′), 3.03 (s, 6H, -N-$(CH_3)_2$), 3.76 (bs, 2H, azep H2′), 4.26 (bs, 2H, azep H7′), 7.65 (s, 1H, pur H8), 12.21 (bs, 1H, pur NH). ^{13}C NMR (125 MHz, DMSO-d_6) δ (ppm): 26.2 (azep C4′, 5′), 26.4 (azep C3′), 29.2 (azep C6′), 37.0 (-N-$(CH_3)_2$), 47.5 (azep C2′), 48.8 (azep C7′), 112.2

(pur C5), 134.7 (pur C8), 153.1 (pur C6), 153.5 (pur C4), 158.9 (pur C2).

*4.1.9. 6-(Azepan-1-yl)-2-(morpholin-4-yl)purine (**9**)*

6-(Azepan-1-yl)-2-chloropurine (**3**; 209 mg, 0.83 mmol) was dissolved in morpholine (2 mL). The solution was heated at 60 °C for 14 h and at 115 °C for 5 h. After cooling, the mixture was refrigerated overnight. The product crystallized from the mixture as a plaster-like substance. The product was filtered off, washed thoroughly with MeOH (10 mL) and dried in a desiccator with P_2O_5. White plaster-like substance. Yield: 221 mg (88%). M.p.: 242–244 °C (>200 °C subl.). HPLC R_t = 13.3 min (75% MeOH + 25% buffer), R_t = 10.6 min (80% MeOH + 20% buffer); UV (80% MeOH + 20% buffer) λ_{max} 245 nm, λ_{min} 275 nm, λ_{max} 290 nm; HPLC purity > 97%. MS ESI + (CV 18) *m/z* (rel. %): 303 $[M+H]^+$ (100); ESI$^-$ (CV 23) *m/z* (rel. %): 301 $[M]^-$ (100). ^{1}H NMR (500 MHz, DMSO-d_6) δ (ppm): 1.47 (bs, 4H, azep H4′, 5′), 1.75 (bs, 4H, azep H3′, 6′), 3.57 (bs, 4H, morph H3′, 5′), 3.62 (bs, 4H, morph H2′, 6′), 3.74 (bs, 2H, azep H2′), 4.28 (bs, 2H, azep H7′), 7.71 (s, 1H, pur H8), 12.31 (bs, 1H, pur NH). ^{13}C NMR (125 MHz, DMSO-d_6) δ (ppm): 26.1 (azep C4′, 5′), 26.4 (azep C3′), 29.1 (azep C6′), 44.8 (morph C3′,5′), 47.6 (azep C2′), 48.8 (azep C7′), 66.1 (morph H2′,6′), 113.0 (pur C5), 135.4 (pur C8), 153.1 (pur C6), 153.2 (pur C4), 158.3 (pur C2).

*4.1.10. 6-(Azepan-1-yl)-8-chloropurine (**10**)*

6-(Azepan-1-yl)-8-chloro-9-(tetrahydropyran-2-yl)purine (**18**; 150 mg, 0.45 mmol) was dissolved in MeOH (6.5 mL). H_2O (0.7 mL) and 10% HCl (6 drops) were added. The solution was stirred at room temperature overnight. The product precipitated after addition of H_2O (5 mL) and conc. NH_4OH (2 drops). The suspension was refrigerated overnight. The product was filtered off, washed thoroughly with H_2O, and briefly with MeOH (2 mL) and diethyl ether. The product was dried at room temperature. White plaster-like substance. Yield: 97 mg (88%). M.p.: 227–228 °C (>200 °C subl.). HPLC R_t = 17.6 min (70% MeOH + 30% buffer); UV (70% MeOH + 30% buffer) λ_{min} 247 nm, λ_{max} 285 nm; HPLC purity > 98%. MS ESI + (CV 17) *m/z* (rel. %): 252 $[M+H]^+$ (100), 254 $[M+H]^+$ (33); ESI$^-$ (CV 22) *m/z* (rel. %): 250 $[M]^-$ (100), 252 $[M+H]^+$ (33). ^{1}H NMR (300 MHz, DMSO-d_6) δ (ppm): 1.47 (bs, 4H, azep H4′, 5′), 1.75 (bs, 4H, azep H3′, 6′), 3.82 (bs, 2H, azep H2′), 4.24 (bs, 2H, azep H7′), 8.20 (s, 1H, pur H2), 13.77 (bs, 1H, pur NH). ^{13}C NMR (75 MHz, DMSO-d_6) δ (ppm): 26.1 (azep C4′, 5′), 26.6 (azep C3′), 28.3 (azep C6′), 47.7 (azep C2′), 49.0 (azep C7′), 119.3 (pur C5), 140.3 (pur C8), 147.8 (pur), 151.0 (pur), 151.9 (pur).

*4.1.11. 6-(Azepan-1-yl)-8-bromopurine (**11**)*

6-(Azepan-1-yl)-8-bromo-9-(tetrahydropyran-2-yl)purine (**19**; 150 mg, 0.39 mmol) was dissolved in MeOH (5 mL). H_2O (0.5 mL) and 10% HCl (5 drops) were added. The solution was stirred at room temperature overnight. The product precipitated after addition of H_2O (16 mL) and conc. NH_4OH (2 drops). The suspension was refrigerated overnight. The product was filtered off, washed thoroughly with H_2O and dried in a desiccator with P_2O_5. Yellowish powder. Yield: 113 mg (98%). M.p.: 215–218 °C (>170 °C subl.). HPLC R_t = 11.8 min (80% MeOH + 20% buffer); UV (80% MeOH + 20% buffer) λ_{min} 247 nm, λ_{max} 285 nm; HPLC purity > 99%. MS ESI + (CV 15) *m/z* (rel. %): 296 $[M+H]^+$ (100), 298 $[M+H]^+$ (100); ESI$^-$ (CV 8) *m/z* (rel. %): 294 $[M]^-$ (98), 296 $[M+H]^+$ (100). ^{1}H NMR (300 MHz, DMSO-d_6) δ (ppm): 1.47 (bs, 4H, azep H4′, 5′), 1.75 (bs, 4H, azep H3′, 6′), 3.81 (bs, 2H, azep H2′), 4.22 (bs, 2H, azep H7′), 8.16 (s, 1H, pur H2), 13.74 (bs, 1H, pur NH). ^{13}C NMR (75 MHz, DMSO-d_6) δ (ppm): 26.1 (azep C4′, 5′), 26.6 (azep C3′), 28.3 (azep C6′), 47.7 (azep C2′), 49.1 (azep C7′), 120.2 (pur C5), 126.8 (pur C8), 149.1 (pur), 151.9 (pur), 152.0 (pur).

*4.1.12. 6-(Azepan-1-yl)-8-methylpurine (**12**)*

6-(Azepan-1-yl)-8-methyl-9-(tetrahydropyran-2-yl)purine (**20**; 260 mg, 0.82 mmol) was dissolved in MeOH (8.2 mL)·H_2O (0.8 mL) and 10% HCl (11 drops) were added. The opalescent solution was kept at room temperature for 10 days·H_2O (15 mL) was added and pH adjusted to 7 with conc. NH_4OH. The slightly opalescent yellowish reaction mixture was refrigerated overnight. The white jelly like substance (first portion of the product) was filtered off, washed with H_2O, then briefly with cold MeOH and diethyl ether. The second portion of the product was obtained by evaporation of ¾ of total volume of the filtrate and by precipitation of the product. The third portion was obtained after evaporation of the 2nd filtrate to dryness. All portions of the product were dried in a desiccator with P_2O_5. White crystals. Yield: 153 mg (80%). M.p.: 198–200 °C (>180 °C subl.). HPLC R_t = 18.2 min (60% MeOH + 40% buffer); UV (60% MeOH + 40% buffer) λ_{min} 239 nm, λ_{max} 280 nm; HPLC purity > 99%. MS ESI + (CV 17) *m/z* (rel. %): 232 $[M+H]^+$ (100); ESI$^-$ (CV 20) *m/z* (rel. %): 230 $[M]^-$ (100). ^{1}H NMR (300 MHz, DMSO-d_6) δ (ppm): 1.46 (bs, 4H, azep H4′, 5′), 1.74 (bs, 4H, azep H3′, 6′), 2.40 (s, 3H, -CH_3), 3.86 (bs, 2H, azep H2′), 4.22 (bs, 2H, azep H7′), 8.08 (s, 1H, pur H2), 12.61 (bs, 1H, pur NH). ^{13}C NMR (75 MHz, DMSO-d_6) δ (ppm): 14.6 (-CH_3), 26.3 (azep C4′, 5′), 27.3 (azep C3′), 28.5 (azep C6′), 48.1 (azep C2′, 7′), 118.5 (pur C5), 146.7 (pur), 151.1 (pur), 152.0 (pur), 152.6 (pur).

*4.1.13. 6-(Azepan-1-yl)-7,9-dihydro-8H-purin-8-one (**13**)*

6-(Azepan-1-yl)-8-benzyloxy-9-(tetrahydropyran-2-yl)purine (synthesis 4.1.21.1.; 200 mg, 0.49 mmol) was dissolved in MeOH (10 mL). 1 M HCl (2 mL) was added and the mixture heated at 45 °C for 3 days. The mixture was diluted with H_2O (5 mL) and pH adjusted to 5 with conc. NH_4OH (10 drops). The stiff white suspension was refrigerated overnight. The product was filtered off, washed thoroughly with H_2O, then briefly with MeOH. The product was dried at room temperature. White crystals. Yield: 114 mg (99%). M.p.: 303–310 °C (decomp.). HPLC R_t = 10.7 min (60% MeOH + 40% buffer); UV (70% MeOH + 30% buffer) λ_{min} 242 nm, λ_{max} 284 nm; HPLC purity > 98%. MS ESI + (CV 38) *m/z* (rel. %): 234 $[M+H]^+$ (100), 256 $[M+Na]^+$ (27), 272 $[M+K]^+$ (18); ESI$^-$ (CV 20) *m/z* (rel. %): 232 $[M]^-$ (100). ^{1}H NMR (300 MHz, DMSO-d_6) δ (ppm): 1.44 (bs, 4H, azep H4′, 5′), 1.68 (bs, 4H, azep H3′, 6′), 3.66 (t, J = 5.8 Hz, 4H, azep H2′, 7′), 7.99 (s, 1H, pur H2), 10.83 (bs, 2H, pur *N*7H, *N*9H). ^{13}C NMR (75 MHz, DMSO-d_6) δ (ppm): 26.3 (azep C4′, 5′), 28.0 (azep C3′, 6′), 47.8 (azep C2′, 7′), 103.7 (pur C5), 146.4 (pur), 149.0 (pur), 150.3 (pur), 153.5 (pur).

*4.1.14. 6-(Azepan-1-yl)-8-methoxypurine (**14**)*

4.1.14.1. 6-(Azepan-1-yl)-8-methoxy-9-(tetrahydropyran-2-yl)purine. Na (40 mg, 1.74 mmol) was dissolved in MeOH (6 mL). 6-(Azepan-1-yl)-8-chloro-9-(tetrahydropyran-2-yl)purine (**18**) (0.30 g, 0.89 mmol) was added. The solution was stirred under Ar at 60 °C for 32 h. After cooling, the mixture was diluted with MeOH (15 mL) and H_2O (5 mL) and pH adjusted to 6 with 1 M HCl. The mixture was concentrated *in vacuo* to total volume of 5 mL and extracted with EtOAc (2 × 20 mL). The EtOAc layer was dried with Na_2SO_4 and evaporated. The residuum was dissolved in hexane (10 mL). Undissolved particles were filtered off. The filtrate was concentrated *in vacuo* and dried in a desiccator with P_2O_5. Viscous white opalescent substance. Yield: 280 mg (94%). HPLC R_t = 15.1 min (85% MeOH + 15% buffer); UV (85% MeOH + 15% buffer) λ_{min} 238 nm, λ_{max} 278 nm; HPLC purity 97%. MS ESI + (CV 17) *m/z* (rel. %): 332 $[M+H]^+$ (100); ESI + (CV 40) *m/z* (rel. %): 332 $[M+H]^+$ (100), 248 $[M-THP+H]^+$ (62). ^{1}H NMR (500 MHz, DMSO-d_6) δ (ppm): 1.41–1.71 (m, 12H), 1.88–1.91 (m, 1H), 2.62–2.70 (m, 1H), 3.54 (bt, J = 11.3 Hz, 3.3 Hz, 1H), 3.86–4.16 (bm, 8H), 5.44 (dd, J = 11.1 Hz, 2.4 Hz, 1H), 8.06 (s, 1H, pur H2). ^{13}C NMR (125 MHz, DMSO-d_6) δ (ppm): 23.3, 25.0, 26.7, 28.5, 48.7, 57.3, 68.3, 81.2, 114.7, 150.4, 150.9, 152.3, 153.7.

*4.1.14.2. 6-(Azepan-1-yl)-8-methoxypurine (**14**)*. 6-(Azepan-1-yl)-8-methoxy-9-(tetrahydropyran-2-yl)purine (synthesis 4.1.14.1; 220 mg, 0.66 mmol) was dissolved in MeOH (6 mL) and 10% HCl (9 drops). H_2O (0.6 mL) was added and the mixture heated at 60 °C for 21 h. The

mixture was diluted with H_2O (5 mL) and pH adjusted to 6 with conc. NH_4OH (1 drop). H_2O (10 mL) was added to enhance the precipitation of the product. The suspension was refrigerated overnight. The product was filtered off, washed thoroughly with H_2O and in a desiccator with P_2O_5. White plaster like substance. Yield: 61 mg (37%). M.p.: 213–216 °C (>170 °C subl.). HPLC R_t = 11.5 min (80% MeOH + 20% buffer); UV (80% MeOH + 20% buffer) λ_{min} 240 nm, λ_{max} 280 nm; HPLC purity 97%. MS ESI+ (CV 47) *m/z* (rel. %): 248 $[M+H]^+$ (100); ESI$^-$ (CV 9) *m/z* (rel. %): 246 $[M]^-$ (100). ^{1}H NMR (300 MHz, DMSO-d_6) δ (ppm): 1.46 (bs, 4H, azep H4′, 5′), 1.74 (bs, 4H, azep H3′, 6′), 3.98 (bs, 7H, azep H2′, 7′, -OCH_3), 8.04 (s, 1H, pur H2), 12.47 (bs, 1H, pur NH). ^{13}C NMR (75 MHz, DMSO-d_6) δ (ppm): 26.2 (azep C4′, 5′), 28.0 (azep C3′, C6′), 48.1 (azep C2′, 7′), 56.0 (-OCH_3), 115.3 (pur C5), 150.2 (pur), 150.7 (pur), 151.5 (pur), 154.7 (pur).

4.1.15. 6-(Azepan-1-yl)-9-methylpurine (15) and 6-(azepan-1-yl)-7-methylpurine (43)

4.1.15.1. 6-Chloro-9-methylpurine and 6-chloro-7-methylpurine. 6-Chloropurine (5 g, 32.35 mmol) was dissolved in DMF (80 mL) and finely pulverized anhydrous K_2CO_3 (8.96 g, 64.83 mmol) was added. The heterogeneous mixture was mixed at room temperature for 3 h while CH_3I (3 × 3.5 mL, 168.66 mmol) was slowly added. The reaction was monitored by TLC ($CHCl_3$:MeOH 9:1). After this time, the reaction mixture was filtered and a small amount of DMF was added. Subsequently, the mixture was concentrated *in vacuo*, crude product was dissolved in EtOAc, and a small portion of distilled H_2O was added. The EtOAc portion was separated, dried over anhydrous Na_2SO_4 and concentrated *in vacuo*. After 12 h, the product was dissolved in 2-PrOH at 50 °C and purified with pulverized coal. The final product was concentrated *in vacuo* and a mixture of two isoforms was obtained. Yield: 3.86 g (71%), HPLC: 89.30% (6Cl9MP) and 10.70% (6Cl7MP). ^{1}H NMR (300 MHz, DMSO-d_6) δ (ppm): 3.86 (s, *N*9-CH_3), 4.07 (s, *N*7-CH_3), 8.65 (s, pur $H8_{6Cl9MP}$), 8.74 (s, pur $H8_{6Cl7MP}$), 8.77 (s, pur H2).

4.1.15.2. 6-(Azepan-1-yl)-9-methylpurine (15) and 6-(azepan-1-yl)-7-methylpurine (43). The crude mixture of 6-chloro-9-methylpurine and 6-chloro-7-methylpurine (synthesis 4.1.15.1; 0.55 g, 3.26 mmol) was dissolved in PrOH (10 mL) together with azepane (0.3 g, 3.02 mmol) and Et_3N (2.0 mL, 14.35 mmol). The mixture was then refluxed at 100 °C. Azepane (0.44 g, 4.44 mmol) was added after 1 h. The mixture was heated for 3 h and then evaporated. The residuum was dissolved in EtOAc, mixed with distilled H_2O and shaken properly. The EtOAc phase was then concentrated *in vacuo*. The mixture of two arisen isoforms (*N*9 and *N*7 methylated derivatives) was dissolved in the mobile phase ($CHCl_3$:MeOH 9:1) (10 mL) and separated on column.

4.1.15.2.1. 6-(Azepan-1-yl)-9-methylpurine (15). Yield: 0.16 g (24%). HPLC purity > 99%. MS ESI+ (CV 20) *m/z* (rel. %): 232.4 (100) $[M+H]^+$. ^{1}H NMR (300 MHz, DMSO-d_6) δ (ppm): 1.47 (bs, 4H, azep), 1.76 (bs, 4H, azep), 3.70 (s, 3H, *N*9-CH_3), 3.82 (bs, 2H, azep); 4.31 (bs, 2H, azep), 8.07 (s, 1H, pur); 8.19 (s, 1H, pur). ^{13}C NMR (125 MHz, DMSO-d_6) δ (ppm): 26.2, 26.6, 28.7, 29.3, 39.5, 47.6, 48.9, 118.6, 140.4, 150.6, 151.9, 153.5.

4.1.15.2.2. 6-(Azepan-1-yl)-7-methylpurine (43). ^{1}H NMR (300 MHz, DMSO-d_6) δ (ppm): 1.54 (bs, 4H, azep), 1.81 (bs, 4H, azep), 3.86–3.71 (m, 4H, azep), 3.95 (s, 3H, *N*7-CH_3), 8.27 (s, 2H, pur H2 and H8). ^{13}C NMR (125 MHz, DMSO-d_6) δ (ppm): 27.2, 27.4, 36.1, 50.5, 113.7, 147.7, 150.5, 153.7, 161.1.

4.1.16. 6-(Azepan-1-yl)-9-(tetrahydropyran-2-yl)purine (16)

6-Chloro-9-(tetrahydropyran-2-yl)purine (prepared from 6-chloropurine according to [43], 5.55 g, 23 mmol) was dissolved in 2-PrOH (60 mL). Et_3N (3.24 mL, 28 mmol) and azepane (3.6 mL, 32 mmol) were added. The solution was heated at 45 °C overnight. The reaction mixture was a suspension of needle crystals and light beige powder. After cooling, the precipitate was filtered off, washed thoroughly with 2-PrOH and H_2O (10 mL) and dried in a desiccator with P_2O_5. Fine white powder. Yield: 5.15 g (74%). M.p.: 163–165 °C. HPLC R_t = 13.6 min (80% CH_3OH + 20% buffer); UV (80% CH_3OH + 20% buffer) λ_{min} 236 nm, λ_{max} 280 nm; HPLC purity > 99%. MS ESI+ (CV 18) *m/z* (rel. %): 302 $[M+H]^+$ (100). ^{1}H NMR (300 MHz, DMSO-d_6) δ (ppm): 1.48 (s, 4H, azep H4′, 5′), 1.55–1.57 (m, 2H, THP H4′, 5′), 1.70–1.77 (m, 5H, azep H3′, 6′, THP 5′), 1.90–1.97 (m, 2H, THP H3′, H4′), 2.17–2.24 (m, 1H, THP H3′), 3.63–3.69 (m, 1H, THP H6′), 3.83 (bs, 2H, azep H2′, 7′), 3.97–4.00 (m, 1H, THP H6′), 4.31 (bs, 2H, azep H2′, 7′), 5.63 (dd, *J* = 11.1, 2.1 Hz, 1H, THP H2′), 8.20 (s, 1H, pur H8), 8.32 (s, 1H, pur H2). ^{13}C NMR (125 MHz, DMSO-d_6) δ (ppm): 22.5, 24.5, 26.2, 26.6, 28.6, 30.1, 47.6, 49.0, 67.7, 80.6, 118.6, 137.7, 149.7, 152.1, 153.5.

4.1.17. 6-(Azepan-1-yl)-9-(β-D-ribofuranosyl)purine (17)

6-Chloropurine riboside (2 g, 6.98 mmol) was dissolved in PrOH (30 mL). Azepane (0.7 g, 7.06 mmol) and Et_3N (4.9 mL, 35.16 mmol) were then added. The mixture was refluxed at 100 °C and monitored by TLC ($CHCl_3$:MeOH 4:1) for 3 h. The reaction mixture was concentrated *in vacuo*. At the end of concentration, distilled H_2O (3 mL) was added to form an azeotropic mixture with PrOH. The evaporated mixture was dissolved in EtOAc and extracted with distilled H_2O. The EtOAc phase was dried over anhydrous Na_2SO_4 and the solvent was evaporated. The residue was washed with Et_2O and placed in a desiccator. Yield: 2.01 g (82%). HPLC purity 99%. MS ESI+ (CV 20) *m/z* (rel. %): 350 (100) $[M+H]^+$. ^{1}H NMR (300 MHz, DMSO-d_6) δ (ppm): 1.48 (bs, 4H, azep), 1.77 (bs, 4H, azep), 3.51–3.56 (m, 1H), 3.62–3.68 (m, 1H), 3.84 (bs, 2H, azep), 3.95 (s, 1H), 4.14 (s, 1H), 4.31 (bs, 2H, azep), 4.60 (q, *J* = 5.6 Hz, 1H), 5.19 (d, *J* = 4.4 Hz, 1H), 5.40 (t, *J* = 5.2 Hz, 1H), 5.46 (d, *J* = 6.0 Hz, 1H), 5.89 (d, *J* = 6.0 Hz, 1H), 8.19 (s, 1H, pur), 8.35 (s, 1H, pur).

4.1.18. 6-(Azepan-1-yl)-8-chloro-9-(tetrahydropyran-2-yl)purine (18)

6-(Azepan-1-yl)-9-(tetrahydropyran-2-yl)purine (**16**) (2.5 g, 8.29 mmol) was dissolved under Ar in dry THF (50 mL). The solution was cooled to −75 °C and a suspension formed. The suspension was treated dropwise with LDA (1 M soln. in hexanes/THF) (13.5 mL, 13.5 mmol) over 10 min. The reaction mixture was further stirred at −75 °C for 1 h 10 min. After this time, a solution of C_2Cl_6 (2 g, 8.45 mmol) in dry THF (10 mL) was added dropwise over 13 min. The reaction mixture was then stirred for 1 h. Then, 20% NH_4Cl (60 mL) was added dropwise. After spontaneous warming to room temperature, the layers were separated. The organic layer was extracted with H_2O (2 × 50 mL), dried with Na_2SO_4, filtered, and evaporated with silica gel (4.31 g). The resulting powder was poured onto a column and purified by column chromatography (mobile phase hexanes:EtOAc 9:1), flow rate 11 mL/min). The product was crystallized from the mobile phase. White crystals. Yield: 2.18 g (78%). M.p.: 87–90 °C. HPLC R_t = 19.3 min (85% MeOH + 15% buffer); UV (85% MeOH + 15% buffer) λ_{min} 241 nm, λ_{max} 281 nm; HPLC purity > 99%. MS ESI+ (CV 17) *m/z* (rel. %): 336 (100) + 338 (37) $[M+H]^+$, ESI+ (CV 27) *m/z* (rel. %): 252 (98) + 254 (33) $[M-THP+H]^+$, 336 (100) + 338 (40) $[M+H]^+$. ^{1}H NMR (300 MHz, DMSO-d_6) δ (ppm): 1.47–1.87 (m, 12H, azep H3′, 4′, 5′, 6′, THP H3′, 4′, 5′), 1.97 (d, *J* = 10.6 Hz, 1H, THP H4′), 2.84 (qd, *J* = 12.4, 4.1 Hz, 1H, THP H3′), 3.64 (td, *J* = 11.1, 4.8 Hz, 1H, THP H6′), 3.82 (bs, 2H, azep H2′, 7′), 4.02 (d, *J* = 11.4 Hz, 1H, THP H6′), 4.16 (bs, 2H, azep H2′, 7′), 5.66 (dd, *J* = 11.3, 2.4 Hz, 1H, THP H2′), 8.21 (s, 1H, pur H2). ^{13}C NMR (75 MHz, DMSO-d_6) δ (ppm): 22.5, 24.4, 26.1, 26.5, 28.0, 28.3, 47.7, 48.9, 68.1, 82.8, 117.3, 134.9, 151.1, 152.2, 152.3.

4.1.19. 6-(Azepan-1-yl)-8-bromo-9-(tetrahydropyran-2-yl)purine (19)

6-(Azepan-1-yl)-9-(tetrahydropyran-2-yl)purine (**16**; 1.5 g, 4.98 mmol) was dissolved under Ar in dry THF (35 mL). The solution was cooled to −75 °C and a suspension formed. The suspension was treated dropwise with LDA (1 M soln. in hexanes/THF; 9 mL, 9 mmol) over 10 min. The reaction mixture was further stirred at −75 °C for 1 h. After this time, a solution of CBr_4 (1.67 g, 5.04 mmol) in dry THF (8 mL)

was added dropwise over 10 min to the reaction mixture, which was then stirred for 2.5 h. Then, 20% NH_4Cl (40 mL) was added dropwise. After spontaneous warming to room temperature, the layers were separated. The organic layer was extracted with H_2O (2 × 40 mL), dried with Na_2SO_4, filtered, and evaporated with silica gel (3 g). The resulting powder was poured onto a column and purified by column chromatography (mobile phase hexanes:EtOAc 9:1, flow rate 11 mL/min). The product was crystallized from the mobile phase. White crystals. Yield: 1.51 g (80%). M.p.: 90–94 °C. HPLC R_t = 18.7 min (85% MeOH + 15% buffer); UV (85% MeOH + 15% buffer) λ_{min} 241 nm, λ_{max} 283 nm; HPLC purity > 99%. MS ESI+ (CV 17) *m/z* (rel. %): 380 (90) + 382 (100) $[M+H]^+$, ESI+ (CV 27) *m/z* (rel. %): 296 (62) + 298 (67) $[M-THP+H]^+$, 380 (88) + 382 (100) $[M+H]^+$. ^{1}H NMR (300 MHz, DMSO-d_6) δ (ppm): 1.47–1.83 (m, 12H, azep H3′, 4′, 5′, 6′, THP H3′, 4′, 5′), 1.97–1.99 (m, 1H, THP H4′), 2.97 (qd, *J* = 12.2, 4.1 Hz, 1H, THP H3′), 3.63 (td, *J* = 11.0, 3.7 Hz, 1H, THP H6′), 3.81 (bs, 2H, azep H2′, 7′), 4.03 (d, *J* = 11.6 Hz, 1H, THP H6′), 4.18 (bs, 2H, azep H2′, 7′), 5.63 (dd, *J* = 11.3, 2.3 Hz, 1H, THP H2′), 8.18 (s, 1H, pur H2). ^{13}C NMR (75 MHz, DMSO-d_6) δ (ppm): 22.6, 24.4, 26.1, 26.6, 28.0, 28.3, 47.7, 48.9, 68.1, 83.9, 119.1, 124.4, 151.5, 152.0, 152.3.

4.1.20. 6-(Azepan-1-yl)-8-methyl-9-(tetrahydropyran-2-yl)purine (**20**)

6-(Azepan-1-yl)-9-(tetrahydropyran-2-yl)purine (**16**; 0.5 g, 1.66 mmol) was dissolved under Ar in dry THF (15 mL). The solution was cooled to −75 °C and a suspension formed. The suspension was treated dropwise with LDA (1 M soln. in hexanes/THF) (3 mL, 2 mmol) over 3 min. The reaction mixture was further stirred at −75 °C for 1 h. After this time, CH_3I (0.1 mL, 1.66 mmol) was added. The reaction mixture was then stirred for 3 h 15 min. The reaction was quenched with 20% NH_4Cl (10 mL) added dropwise. After spontaneous warming to room temperature, the layers were separated. The organic layer was extracted with H_2O (2 × 10 mL), dried with Na_2SO_4, filtered, and evaporated. The viscous crude product was dried in a desiccator until it became crystalline. The solid product was crystallized from hexanes/EtOAc. White crystals. Yield: 427 mg (82%). M.p.: 116–119 °C. HPLC R_t = 13.7 min (85% MeOH + 15% buffer); UV (80% MeOH + 20% buffer) λ_{min} 239 nm, λ_{max} 279 nm; HPLC purity 99%. MS ESI+ (CV 17) *m/z* (rel. %): 316 (100) $[M+H]^+$. ^{1}H NMR (300 MHz, DMSO-d_6) δ (ppm): 1.46–1.74 (m, 12H, azep H3′, 4′, 5′, 6′, THP H3′, 4′, 5′), 1.92–1.96 (m, 1H, THP H4′), 2.51–2.53 (m overlapped with DMSO-d_6, 1H, THP H3′), 2.57 (s, 1H, -CH_3), 3.65 (td, *J* = 11.0, 3.7 Hz, 1H, THP H6′), 3.82 (bs, 2H, azep H2′, 7′), 4.03 (d, *J* = 11.5 Hz, 1H, THP H6′), 4.27 (bs, 2H, azep H2′, 7′), 5.66 (dd, *J* = 11.3, 2.2 Hz, 1H, THP H2′), 8.13 (s, 1H, pur H2). ^{13}C NMR (75 MHz, DMSO-d_6) δ (ppm): 15.3, 22.7, 24.6, 26.2, 26.6, 28.6, 29.2, 47.9, 48.6, 68.1, 82.0, 117.4, 147.0, 151.0, 151.1, 152.7.

4.1.21. 6-(Azepan-1-yl)-9-(tetrahydropyran-2-yl)-7,9-dihydro-8H-purin-8-one (21)

Na (0.16 g, 6.96 mmol) was dissolved in benzyl alcohol (6 mL). 6-(Azepan-1-yl)-8-chloro-9-(tetrahydropyran-2-yl)purine (**18**; 0.45 g, 1.34 mmol) was added. The solution was stirred under Ar at 90 °C overnight. Then, the mixture was evaporated at p = 0.5 mbar, t = 100 °C. The residuum was dissolved in MeOH (6.5 mL), H_2O (11 mL) and acidified with AcOH (0.5 mL). The mixture was evaporated. The residuum was mixed with H_2O (6 mL) and extracted with EtOAc (3 × 6 mL). The EtOAc portions were dried over Na_2SO_4. Na_2SO_4 was filtered off and the filtrate was evaporated. The residuum was mixed with hexanes:EtOAc 9:1 (3–4 mL) and subjected to column chromatography (mobile phase hexanes:EtOAc 9:1, flow rate 11 mL/min). Column chromatography provided two products:

4.1.21.1. 6-(Azepan-1-yl)-8-benzyloxy-9-(tetrahydropyran-2-yl) purine.

White viscous substance. Yield: 0.2 g (37%). TLC R_f = 0.16 (hexanes:EtOAc 9:1). MS ESI+ (CV 17) *m/z* (rel. %): 408 (100) $[M+H]^+$, ESI+ (CV 27) *m/z* (rel. %): 324 (27) $[M-THP+H]^+$, 408 (100) $[M+H]^+$. ^{1}H NMR (500 MHz, DMSO-d_6) δ (ppm): 1.42 (s, 4H, azep H4′, 5′), 1.45–1.50 (m overlapped, 2H, THF), 1.54–1.65 (m overlapped, 1H, THP), 1.71 (s, 4H, azep H3′, 6′), 1.65–1.76 (m overlapped, 1H, THP), 1.85–1.93 (m, 1H, THP H4′), 2.67 (dq, *J* = 12.3, 4.0 Hz, 1H, THP H3′), 3.55 (m, 1H, THP H6′), 3.80 (bs, 2H, azep H2′, 7′), 3.94 (d, *J* = 13.0 Hz, 1H, THP H6′), 4.06 (bbs, 2H, azep H2′, 7′), 5.44 (m, 3H, THP H2′, -OCH_2-), 7.29–7.33 (m, 1H, Bn), 7.34–7.39 (m, 2H, Bn), 7.45–7.50 (m, 2H, Bn), 8.07 (s, 1H, pur H2). ^{13}C NMR (75 MHz, DMSO-d_6) δ (ppm): 23.3, 25.1, 26.7 (2x), 27.8 (bs), 28.6, 29.5 (bs), 48.8, 48.9, 68.3, 71.5, 81.2, 114.7, 128.7 (2x), 128.8, 128.9 (2x), 136.3, 150.3, 151.0, 152.2, 152.9.

4.1.21.2. 6-(Azepan-1-yl)-9-(tetrahydropyran-2-yl)-7,9-dihydro-8H-purin-8-one (21).

White powder. Yield: 63.2 mg (15%). M.p.: 258–263 °C. HPLC R_t = 14.1 min (70% MeOH + 30% buffer); UV (70% MeOH + 30% buffer) λ_{min} 242 nm, λ_{max} 284 nm; HPLC purity > 99%. MS ESI+ (CV 17) *m/z* (rel. %): 318 (100) $[M+H]^+$. ^{1}H NMR (300 MHz, DMSO-d_6) δ (ppm): 1.44–1.68 (m, 12H, azep H3′,4′, 5′, 6′, THP H3′, 4′, 5′), 1.90–1.93 (m, 1H, THP H4′), 2.85–2.98 (m, 1H, THP H3′), 3.53 (td, *J* = 11.0, 3.7 Hz, 1H, THP H6′), 3.67 (t, *J* = 6.0 Hz, 4H, azep H2′, 7′), 3.94 (d, *J* = 11.3 Hz, 1H, THP H6′), 5.35 (dd, *J* = 11.4, 2.0 Hz, 1H, THP H2′), 8.07 (s, 1H, pur H2), 10.72 (s, 1H, pur *N*7H). ^{13}C NMR (75 MHz, DMSO-d_6) δ (ppm): 23.0, 24.6, 26.3 (2x), 27.2, 27.9 (2x), 47.9 (2x), 67.7, 79.9, 102.7, 146.8, 147.9, 150.2, 152.0.

4.1.22. 6-(Piperidin-1-yl)purine (**22**)

6-Chloropurine (1 g, 6.47 mmol) was refluxed with piperidine (4.5 mL, 65.77 mmol) in PrOH at 80–90 °C for 3 hrs. The reaction was monitored *via* TLC ($CHCl_3$:MeOH 4:1). After completion, the reaction mixture was evaporated. The residue was dissolved in EtOAc and mixed with distilled H_2O. EtOAc was dried over Na_2SO_4, filtered, and evaporated. Crude product was air-dried. Yield: 1.2 g (91%). HPLC purity > 99%. MS ESI+ (CV 17) *m/z* (rel. %): 204 (100) $[M+H]^+$. ^{1}H NMR (500 MHz, DMSO-d_6) δ (ppm): 1.53–1.58 (m, 4H), 1.64–1.68 (m, 2H), 4.18 (s, 4H), 8.07 (s, 1H), 8.16 (s, 1H), 12.96 (s, 1H). ^{13}C NMR (125 MHz, DMSO-d_6) δ (ppm): 24.3, 25.7, 45.6, 118.6, 137.7, 151.3, 151.8, 153.1.

4.1.23. 6-(Piperidin-1-yl)-9-(tetrahydropyran-2-yl)purine (**23**)

6-Chloro-9-(tetrahydropyran-2-yl)purine (prepared from 6-chloropurine according to [43], 2.0 g, 8.38 mmol) was dissolved in PrOH. Piperidine (1.0 mL, 10.1 mmol) and Et_3N (5.0 mL, 35.8 mmol) were added. The mixture was refluxed at 90 °C for 3 hrs and monitored by TLC ($CHCl_3$:MeOH 4:1). The final mixture was evaporated and diethylether was added. Emerging white crystals were collected. Yield: 2.05 g (85%). HPLC purity > 99%. MS ESI+ (CV 18) *m/z* (rel. %): 288 $[M+H]^+$ (100). ^{1}H NMR (500 MHz, DMSO-d_6) δ (ppm): 1.55–1.57 (m, 6H), 1.64–1.76 (m, 3H), 1.89–1.96 (m, 2H), 2.20 (tdd, *J* = 12.9, 10.9, 3.8 Hz, 1H), 3.63–3.69 (m, 1H), 3.97–4.01 (m, 1H), 4.17 (bs, 4H), 5.64 (dd, *J* = 11.1, 2.2 Hz, 1H), 8.20 (s, 1H), 8.33 (s, 1H). ^{13}C NMR (125 MHz, DMSO-d_6) δ (ppm): 22.5, 24.2, 24.5, 25.7, 30.1, 67.7, 80.7, 118.7, 137.4, 149.9, 152.0, 153.1.

4.1.24. 6-(Piperidin-1-yl)-9-(β-D-ribofuranosyl)purine (**24**)

6-Chloropurine riboside (2 g, 6.98 mmol) was dissolved in PrOH (30 mL). Piperidine hydrochloride (0.9 g, 7.4 mmol) and Et_3N (6 mL, 43.05 mmol) were then added. The mixture was refluxed at 100 °C for 2 h and then evaporated. The residue was dissolved in EtOAc and distilled H_2O was added. The emerged precipitate was filtered off, washed with distilled H_2O, and air-dried. Yield: 0.93 g (40%). HPLC purity > 99%. MS ESI+ (CV 20) *m/z* (rel. %): 336.4 (100) $[M+H]^+$. ^{1}H NMR (500 MHz, DMSO-d_6) δ (ppm): 1.55–1.58 (m, 4H, piper), 1.65–1.68 (m, 2H, piper), 3.54 (ddd, *J* = 12.0, 7.0, 3.6 Hz, 1H), 3.66 (ddd, *J* = 12.1, 4.5, 3.6 Hz, 1H), 3.95 (q, *J* = 3.5 Hz, 1H), 4.13 (td, *J* = 4.8, 3.5 Hz, 1H), 4.19 (bs, 4H), 4.57 (td, *J* = 6.1, 4.9 Hz, 1H), 5.18 (d, *J* = 4.6 Hz,

1H); 5.36 (dd, J = 7.0, 4.5 Hz, 1H), 5.45 (d, J = 6.2 Hz, 1H), 5.89 (d, J = 5.9 Hz, 1H); 8.20 (s, 1H, pur), 8.36 (s, 1H, pur). ^{13}C NMR (125 MHz, DMSO-d_6) δ (ppm): 24.2, 25.7, 61.5, 70.5, 73.4, 85.8, 87.8, 119.5, 138.5, 150.1, 151.8, 153.1.

*4.1.25. 6-(4-Hydroxypiperidin-1-yl)purine (**25**)*

6-Chloropurine (0.7 g, 4.53 mmol) was dissolved in PrOH (30 mL). 4-Hydroxypiperidine (0.6 g, 5.93 mmol) and Et_3N (2 mL, 14.35 mmol) were then added. The mixture was refluxed at 100 °C and monitored by TLC ($CHCl_3$:MeOH 4:1) for 1.5 h. The emerged crystalline solid was filtered off, washed with distilled H_2O, and air-dried. Yield: 0.6 g (60%). HPLC purity > 99%. MS ESI+ (CV 20) m/z (rel. %): 220.4 (100) $[M+H]^+$. ^{1}H NMR (500 MHz, DMSO-d_6) δ (ppm): 1.23–1.48 (m, 2H), 1.81 (s, 2H), 3.59 (s, 2H), 3.77 (s, 1H), 4.60–5.04 (m, 3H), 8.09 (s, 1H), 8.18 (s, 1H), 12.99 (s, 1H).

*4.1.26. 1-(Purin-6-yl)piperidin-4-one (**26**)*

6-Chloropurine (0.2 g; 1.29 mmol) was dissolved in DMF (5 mL). Et_3N (0.44 mL, 3.15 mmol) and 4-piperidone monohydrate hydrochloride (276 mg, 1.77 mmol) were added. The solution was heated at 50 °C for 2 h. After cooling, the reaction mixture was refrigerated for 2 d. The resulting solid substance was filtered off and washed with distilled H_2O. Glassy crystals were dissolved and yellow powder remained (portion I of the product, m = 45 mg). The filtrate was evaporated, the residuum was adsorbed on silica gel (1 g) and purified by column chromatography (mobile phase $CHCl_3$:MeOH:NH_4OH 95:5:0.5, flow rate 10 mL/min). Combined fractions with the product were partly evaporated to a total volume 15–20 mL and refrigerated for 4 d. The emerging crystals were filtered off and air-dried (portion II of the product, m = 72 mg). The filtrate was evaporated to dryness (portion III of the product, m = 0.1 g). White powder. Yield: 216 mg (77%). M.p.: 280–285 °C. HPLC R_t = 8.8 min (broad peak, R_t = 6.7–9.9 min) (40% MeOH + 60% buffer); UV (60% MeOH + 40% buffer) λ_{min} 234 nm, λ_{max} 277 nm. HPLC purity 98% (portion II). MS ESI+ (CV 13) m/z (rel. %): 218 $[M+H]^+$ (47), 250 $[M+CH_3OH+H]^+$ (100); ESI$^-$ (CV 20) m/z (rel. %): 216 $[M]^-$ (100), 248 $[M+CH_3OH]^-$ (32). ^{1}H NMR (500 MHz, DMSO-d_6) δ (ppm): 2.53 (bs, 4H, piper H3, H5), 4.45 (bs, 4H, piper H2, H6), 8.20 (s, 1H, pur H8′), 8.30 (s, 1H, pur H2′), 13.15 (bs, 1H, pur NH). ^{13}C NMR (125 MHz, DMSO-d_6) δ (ppm): 40.7 (piper C3, C5), 43.7 (piper C2, C6), 119.1 (pur C5′), 138.6 (pur C8′), 151.5 (pur C4′), 151.9 (pur C2′), 152.9 (pur C6′), 207.5 (piper C4).

*4.1.27. 1-(2-Chloropurin-6-yl)piperidin-4-one (**27**)*

2,6-Dichloropurine (0.51 g; 2.7 mmol) was dissolved in 2-PrOH (8 mL). Et_3N (0.84 mL, 6 mmol) and 4-piperidone monohydrate hydrochloride (502 mg, 3.28 mmol) were added. The solution was heated at 60 °C for 2 h. After cooling, the pH of the reaction mixture was adjusted with acetic acid (15 drops) to pH = 6. The suspension was refrigerated overnight. The precipitate was filtered off, washed thoroughly with 2-PrOH (4 mL) and distilled H_2O (10 mL), and dried in a desiccator with P_2O_5. White plaster-like solid. Yield: 514 mg (76%). M.p.: 283–286 °C. HPLC R_t = 7.7 min (broad peak, R_t = 5.6–9.0 min) (60% MeOH + 40% buffer); UV (60% MeOH + 40% buffer) λ_{min} 238 nm, λ_{max} 278 nm. HPLC purity > 98%. MS ESI+ (CV 18) m/z (rel. %): 252 $[M+H]^+$ (44), 254 $[M+H]^+$ (18), 284 $[M+CH_3OH+H]^+$ (96), 286 $[M+CH_3OH+H]^+$ (34), 306 $[M+CH_3OH+Na]^+$ (100), 308 $[M+CH_3OH+Na]^+$ (33); ESI$^-$ (CV 19) m/z (rel. %): 250 $[M]^-$ (100), 252 $[M]^-$ (34), 282 $[M+CH_3OH]^-$ (42), 284 $[M+CH_3OH]^-$ (16). ^{1}H NMR (500 MHz, DMSO-d_6) δ (ppm): 2.50 (t, J = 6.2 Hz, 4H), 4.45 (bs, 4H), 8.17 (s, 1H), 13.24 (bs, 1H). ^{13}C NMR (125 MHz, DMSO-d_6) δ (ppm): 40.3, 43.5 (bs), 118.0, 139.1, 152.4, 152.6, 153.3, 207.1.

*4.1.28. 1-[9-(Tetrahydropyran-2-yl)purin-6-yl]piperidin-4-one (**28**)*

6-Chloro-9-(tetrahydropyran-2-yl)purine (prepared from 6-chloropurine according to [43], 1.3 g, 5.45 mmol) was dissolved in 2-PrOH (20 mL). Et_3N (1.66 mL, 11.90 mmol) and 4-piperidone monohydrate hydrochloride (1 g, 6.51 mmol) were added. The mixture was stirred at room temperature for 6 days. The mixture was evaporated. The residuum was dissolved in distilled H_2O (30 mL) and EtOAc (30 mL). After extraction, the EtOAc layer was dried with Na_2SO_4, evaporated and dried in a desiccator with P_2O_5. The crude product (1.52 g, 93%) was crystallized from EtOAc (8 mL). White crystals. Yield: 0.59 g (36%). M.p.: 136–138 °C. HPLC R_t = 11.0 min (60% MeOH + 40% buffer); UV (70% MeOH + 30% buffer) λ_{min} 235 nm, λ_{max} 278 nm. HPLC purity > 99%. MS ESI+ (CV 18) m/z (rel. %): 334 $[M+H+MeOH]^+$ (100), 302 $[M+H]^+$ (46). ^{1}H NMR (500 MHz, DMSO-d_6) δ (ppm): 1.57–1.60 (m, 2H, THP H5′), 1.71–1.76 (m, 1H, THP H4′), 1.91–1.98 (m, 2H, THP H3′, H4′), 2.20–2.26 (m, 1H, THP H3′), 2.46 (t, J = 6.1 Hz, 4H, piper H3′, H5′), 3.67 (dt, J = 11.0, 4.0 Hz, 1H, THP H6′), 3.98–4.02 (m, 1H, THP H6′), 4.48 (bs, 4H, piper H2, H6), 5.68 (dd, J = 11.0, 2.0 Hz, 1H, THP H2′), 8.31 (s, 1H, pur H2′), 8.42 (s, 1H, pur H8′). ^{13}C NMR (125 MHz, DMSO-d_6) δ (ppm): 22.4 (THP C4′), 24.5 (THP C5′), 30.1 (THP C3′), 40.6 (piper C3, C5), 43.7 (piper C2, C6), 67.7 (THP C6′), 80.8 (THP C2′), 119.2 (pur C5′), 138.3 (pur C8′), 150.1 (pur C4′), 152.1 (pur C2′), 153.0 (pur C6′), 207.4 (piper C4).

*4.1.29. 1-(Purin-6-yl)piperidine-4-carboxamide (**29**)*

6-Chloropurine (0.1 g, 0.65 mmol) was dissolved in PrOH. 4-Piperidinecarboxamide (0.99 g, 7.72 mmol) and Et_3N (0.5 mL, 3.58 mmol) was added. The mixture was refluxed at 90 °C for 3 hrs and monitored by TLC ($CHCl_3$:MeOH 4:1). The final mixture was concentrated. Et_2O was added. The resulting yellowish crystals were collected. Yield: 136 mg (85%). HPLC purity > 99%. MS ESI+ (CV 18) m/z (rel. %): 247 $[M+H]^+$ (100). ^{1}H NMR (300 MHz, DMSO-d_6) δ (ppm): 1.52 (qd, J = 12.4, 4.2 Hz, 2H), 1.79 (dd, J = 13.4, 3.7 Hz, 2H), 2.42–2.47 (m, 1H), 3.12 (m, 2H), 5.32 (bs, 2H), 6.80 (s, 1H), 7.32 (s, 1H), 8.12 (s, 1H), 8.20 (s, 1H), 13.0 (bs, 1H). ^{13}C NMR (125 MHz, DMSO-d_6) δ (ppm): 28.4, 41.7, 44.5, 118.6, 138.3, 151.1, 151.4, 152.9, 176.1.

*4.1.30. 6-(4-Methoxycarbonylpiperidin-1-yl)purine (**30**)*

6-Chloropurine (0.59 g, 3.82 mmol) was dissolved in PrOH (30 mL). Methyl 4-piperidinecarboxylate (0.7 g, 4.89 mmol) and Et_3N (1.6 mL, 11.48 mmol) was then added. The mixture was refluxed at 100 °C and monitored by TLC ($CHCl_3$:MeOH 9:1) for 5.5 h. The resulting mixture was evaporated to half the volume, and the crystals of the final product occurred after the solution was cooled. The crystals were filtered off, washed with distilled H_2O, and air-dried. Yield: 0.7 g (70%). HPLC purity 98%. MS ESI+ (CV 20) m/z (rel. %): 262.4 (100) $[M+H]^+$. ^{1}H NMR (500 MHz, CD_3OD) δ (ppm): 1.69–1.77 (m, 2H), 2.04 (dd, J = 13.3, 3.8 Hz, 2H), 2.77 (tt, J = 11.0, 4.0 Hz, 1H), 3.34–3.40 (m, 2H), 3.69 (s, 3H), 5.24 (d, J = 12.6 Hz, 2H), 8.00 (s, 1H), 8.20 (s, 1H). ^{13}C NMR (125 MHz, CD_3OD) δ (ppm): 29.3, 42.2, 45.8, 52.2, 120.3, 139.0, 153.0, 155.0, 176.6.

*4.1.31. 6-(1,4-Dioxa-8-azaspiro[4.5]decan-8-yl)purine (**31**)*

6-Chloropurine (200 mg, 1.29 mmol) was dissolved in DMF (5 mL). Et_3N (0.22 mL, 1.56 mmol) and 1,4-dioxa-8-azaspiro[4.5]decane (0.18 mL, 1.42 mmol) were added. The solution was heated at 50 °C overnight. After cooling, the pH of the mixture was adjusted with acetic acid (10 drops) to pH = 7. The suspension was refrigerated overnight. The resulting precipitate was filtered off, washed thoroughly with distilled H_2O, and dried in a desiccator with P_2O_5. White powder. Yield: 207 mg (61%). M.p.: 280–283 °C. HPLC R_t = 8.7 min (60% MeOH + 40% buffer); UV (60% MeOH + 40% buffer) λ_{min} 234 nm, λ_{max} 277 nm. HPLC purity > 99%. MS ESI+ (CV 18) m/z (rel. %): 262 $[M+H]^+$ (100); ESI$^-$ (CV 19) m/z (rel. %): 260 $[M]^-$ (100). ^{1}H NMR (500 MHz, DMSO-d_6) δ (ppm): 1.66–1.68 (m, 4H, piperidine H3′, H5′), 3.91 (s, 4H, dioxolane H4′, H5′), 4.27 (bs, 4H, piperidine H2′, H6′), 8.10 (s, 1H, pur H8), 8.19 (s, 1H, pur H2), 13.00 (bs, 1H, pur N9H). ^{13}C NMR (125 MHz, DMSO-d_6) δ (ppm): 34.7 (piperidine C3′, C5′), 42.7 (bs, piperidine C2′, C6′), 63.8 (dioxolane C4′, C5′), 106.5 (spiro C), 118.8 (pur

C5), 138.1 (pur C8), 151.4 (pur C4), 151.8 (pur C2), 152.9 (pur C6).

4.1.32. 2-(2-Hydroxyethylamino)-6-(1,4-dioxa-8-azaspiro[4.5]decan-8-yl)purine (32)

2-Chloro-6-(1,4-dioxa-8-azaspiro[4.5]decan-8-yl)purine (**33**; 143 mg, 0.49 mmol) was dissolved in ethanolamine (1.5 mL). The solution was heated at 147 °C for 25 h. After cooling, the reaction mixture was refrigerated for one week. During this time, the product solidified. The solid was filtered off, washed thoroughly with cold 2-PrOH (10 mL) and distilled H_2O (10 mL), and dried in a desiccator with P_2O_5. White plaster-like solid. Yield: 120 mg (78%). M.p.: 246–248 °C. HPLC Rt = 5.4 min (60% MeOH + 40% buffer), Rt = 6.9 min (50% MeOH + 50% buffer); UV (50% MeOH + 50% buffer) λ_{max} 238 nm, λ_{min} 251 nm, λ_{max} 255 nm, λ_{min} 273 nm, λ_{max} 291 nm. HPLC purity 100%. MS ESI+ (CV 18) *m/z* (rel. %): 321 $[M+H]^+$ (100); ESI$^-$ (CV 19) *m/z* (rel. %): 319 $[M]^-$ (100). ^{1}H NMR (500 MHz, DMSO-d_6) δ (ppm): 1.63–1.65 (m, 4H), 3.28 (q, J = 6.1 Hz, 2H), 3.50 (t, J = 6.1 Hz, 2H), 3.91 (s, 4H), 4.19 (bs, 4H), 4.63 (bs, 1H), 6.09 (t, J = 5.8 Hz, 1H), 7.66 (s, 1H), 12.27 (bs, 1H). ^{13}C NMR (125 MHz, DMSO-d_6) δ (ppm): 34.7, 42.4, 43.9, 60.3, 63.8, 106.6, 113.2, 134.6, 153.1, 153.7, 158.8.

4.1.33. 2-Chloro-6-(1,4-dioxa-8-azaspiro[4.5]decan-8-yl)purine (33)

2,6-Dichloropurine (206 mg, 1.09 mmol) was dissolved in 2-PrOH (3 mL). Et_3N (0.23 mL, 1.63 mmol) and 1,4-dioxa-8-azaspiro[4.5]decane (0.17 mL, 1.30 mmol) were added. The solution, which soon became a suspension, was heated at 65 °C for 1.5 h. After cooling, the pH of the mixture was adjusted with acetic acid (10 drops) to pH = 7. The suspension was refrigerated overnight. The precipitate was filtered off, washed thoroughly with 2-PrOH and distilled H_2O, and dried in a desiccator with NaOH. White plaster-like solid. Yield: 280 mg (87%). M.p.: 275–278 °C. HPLC R_t = 16.9 min (60% MeOH + 40% buffer); UV (60% MeOH + 40% buffer) λ_{min} 238 nm, λ_{max} 278 nm. HPLC purity 100%. MS ESI+ (CV 18) *m/z* (rel. %): 296 $[M+H]^+$ (74), 298 $[M+H]^+$ (27), 318 $[M+Na]^+$ (100), 320 $[M+Na]^+$ (38); ESI$^-$ (CV 19) *m/z* (rel. %): 294 $[M]^-$ (100), 296 $[M]^-$ (31). ^{1}H NMR (500 MHz, DMSO-d_6) δ (ppm): 1.70–1.73 (m, 4H), 3.93 (s, 4H), 4.25 (bs, 4H), 8.08 (s, 1H), 13.05 (bs, 1H). ^{13}C NMR (125 MHz, DMSO-d_6) δ (ppm): 34.6, 42.2 (bs from HMBC), 63.9, 106.3, 117.7, 138.7, 152.4, 152.6, 153.1.

4.1.34. 6-(1,4-Dioxa-8-azaspiro[4.5]decan-8-yl)-9-(tetrahydropyran-2-yl)purine (34)

6-Chloro-9-(tetrahydropyran-2-yl)purine (prepared from 6-chloropurine according to [43], 0.95 g, 3.98 mmol) was dissolved in 2-PrOH (20 mL), and Et_3N (0.67 mL, 4.80 mmol) and 1,4-dioxa-8-azaspiro[4.5]decane (0.61 mL, 4.76 mmol) were added. The solution was stirred at room temperature for 1 d and then evaporated. The residuum was dissolved in distilled H_2O (20 mL) and EtOAc (50 mL). The mixture was shaken in a separating funnel. The resulting solid particles were filtered off (portion I of the product, m = 0.15 g). Brine (10 mL) was added to the filtrate. After shaking, the EtOAc layer was separated and extracted with brine (2 × 20 mL). Brine layers were re-extracted with EtOAc (20 mL). Combined EtOAc layers were dried with Na_2SO_4. Na_2SO_4 was filtered off, and the filtrate was concentrated to 4 mL volume, inoculated with crystals from portion I, and refrigerated for 6 d. The resulting crystals were filtered off, washed briefly with cold EtOAc and air-dried (portion II of the product, m = 0.62 g). Precipitation with hexanes from the filtrate produced portion III of the product (m = 0.34 g). White crystals. Overall yield: 1.11 g (81%). M.p.: 113–118 °C. HPLC R_t = 13.4 min (70% MeOH + 30% buffer); UV (80% MeOH + 20% buffer) λ_{min} 235 nm, λ_{max} 278 nm. HPLC purity > 99%. MS ESI+ (CV 23) *m/z* (rel. %): 346 $[M+H]^+$ (100). ^{1}H NMR (500 MHz, DMSO-d_6) δ (ppm): 1.54–1.58 (m, 2H, THP H5′), 1.67–1.72 (m, 5H, piperidine H3′, H5′, THP H4′), 1.89–1.96 (m, 2H, THP H3′, H4′), 2.20 (dq, J = 12.0 Hz, 3.3 Hz, 1H, THP H3′), 3.66 (td, J = 11.0 Hz, 3.7 Hz, 1H, THP H6′), 3.92 (s, 4H, dioxolane H4′, H5′), 3.95–4.01 (m, 1H, THP H6′), 4.27 (bs, 4H, piper H2′, H6′), 5.64 (dd, J = 10.7, 2.2 Hz, 1H, THP H2′), 8.23 (s, 1H, pur H2), 8.36 (s, 1H, pur H8). ^{13}C NMR (125 MHz, DMSO-d_6) δ (ppm): 22.4 (THP C4′), 24.5 (THP C5′), 30.1 (THP C3′), 34.7 (piperidine C3′, C5′), 42.8 (bs, piperidine C2′, C6′), 63.8 (dioxolane C4′, C5′), 67.7 (THP C6′), 80.8 (THP C2′), 106.5 (spiro C), 118.9 (pur C5), 137.8 (pur C8), 150.0 (pur C4), 152.0 (pur C2), 152.9 (pur C6).

4.1.35. 6-(1-Oxa-4-thia-8-azaspiro[4.5]decan-8-yl)purine (35)

1-(Purin-6-yl)piperidin-4-one (**26**; 193 mg, 0.89 mmol) was mixed with toluene (10 mL), mercaptoethanol (81 µL, 1.15 mmol), and *p*-toluenesulfonic acid monohydrate (165 mg, 0.87 mmol). The suspension was heated at 104 °C for 4 h. Dehydration was ensured by continuous azeotropic distillation. The reaction mixture was a suspension of white precipitate and dark solid on the bottom of the flask in clear liquid. The reaction mixture was mixed with $CHCl_3$ to dissolve solid particles, then extracted with 0.25% Na_2CO_3. The organic layer was dried with Na_2SO_4 and evaporated. The residuum was dissolved in MeOH, adsorbed on silica gel (1.44 g), and purified by column chromatography (mobile phase $CHCl_3$:MeOH:NH_4OH 92.5:7.5:0.75, flow rate 10 mL/min). White crystals. Yield: 148 mg (60%). M.p.: 283–284 °C. HPLC R_t = 10.7 min (70% MeOH + 30% buffer); UV (70% MeOH + 30% buffer) λ_{min} 234 nm, λ_{max} 278 nm. HPLC purity 99%. MS ESI+ (CV 18) *m/z* (rel. %): 278 $[M+H]^+$ (100), 300 $[M+Na]^+$ (12); ESI$^-$ (CV 19) *m/z* (rel. %): 276 $[M]^-$ (100). ^{1}H NMR (300 MHz, DMSO-d_6) δ (ppm): 1.95 (t, J = 5.6 Hz, 4H, piperidine H3′, H5′), 3.07 (t, J = 6.0 Hz, 2H, SCH_2-), 4.16 (bs, cv, 2H, piperidine H2′, H6′), 4.16 (t, J = 6.0 Hz, cv, 2H, OCH_2-), 4.40 (bs, 2H, piperidine H2′, H6′), 8.11 (1H, s, pur H8), 8.20 (s, 1H, pur H2), 13.03 (1H, bs, pur NH). ^{13}C NMR (75 MHz, DMSO-d_6) δ (ppm): 32.5 (piperidine C3′, C5′), 38.9 (oxathiolane C4′, cv with DMSO-d_6), 43.2 (bs, piperidine C2′, C6′), 69.4 (oxathiolane C5′), 93.6 (spiro C), 118.8 (pur C5), 138.1 (pur C8), 151.4 (pur C4), 151.7 (pur C2), 152.8 (pur C6).

4.1.36. 6-(1,4-Dithia-8-azaspiro[4.5]decan-8-yl)purine (36)

1-(Purin-6-yl)piperidin-4-one (**26**) (209 mg, 0.96 mmol) was mixed with toluene (10 mL), 1,2-ethanedithiol (155 µL, 1.85 mmol), and *p*-toluenesulfonic acid monohydrate (268 mg, 1.41 mmol). The suspension was heated at 104 °C for 6 h. Dehydration was ensured by continuous azeotropic distillation. The reaction mixture was a suspension of dark solid on the bottom of the flask in clear rust-coloured liquid. The reaction mixture was mixed with $CHCl_3$ to dissolve the solid, then shaken with 0.25% Na_2CO_3. The organic layer was dried with Na_2SO_4 and evaporated. The residuum was dissolved in MeOH, adsorbed on silica gel (1.57 g), and purified by column chromatography (gradient elution starting with mobile phase $CHCl_3$:MeOH 99.5:0.5, ending with $CHCl_3$:MeOH 97.5:2.5, flow rate 10 mL/min). The post-chromatography product (234 mg, 83%) was crystallized from $CHCl_3$:MeOH 55:45. White crystals. Yield: 48 mg (17%). M.p.: 314–320 °C. HPLC R_t = 17.3 min (70% MeOH + 30% buffer); UV (70% MeOH + 30% buffer) λ_{min} 235 nm, λ_{max} 279 nm. HPLC purity 100%. MS ESI+ (CV 18) *m/z* (rel. %): 294 $[M+H]^+$ (100); ESI$^-$ (CV 19) *m/z* (rel. %): 292 $[M]^-$ (100). ^{1}H NMR (300 MHz, DMSO-d_6) δ (ppm): 2.07–2.11 (m, 4H, piperidine H3′, H5′), 3.34 (s, 4H, dithiolane H4′, H5′), 4.29 (bs, 4H, piper H2′, H6′), 8.11 (s, 1H, pur H8), 8.20 (s, 1H, pur H2), 13.02 (bs, 1H, pur NH). ^{13}C NMR (75 MHz, DMSO-d_6) δ (ppm): 37.9 (piperidine C3′, C5′), 41.4 (dithiolane C4′, C5′), 44.6 (bs, piperidine C2′, C6′), 66.5 (spiro C), 118.8 (pur C5), 138.1 (pur C8), 151.4 (pur C4), 151.7 (pur C2), 152.8 (pur C6).

4.1.37. 2-Chloro-6-(1,4-dithia-8-azaspiro[4.5]decan-8-yl)purine (37)

1-(2-Chloropurin-6-yl)piperidin-4-one (**27**; 215 mg, 1.00 mmol) was suspended in toluene (10 mL). 1,2-Ethanedithiol (0.11 mL, 1.31 mmol) and *p*-toluenesulfonic acid monohydrate (198 mg, 1.04 mmol) were added. The reaction mixture was heated at 90 °C for 3 h 40 min. After cooling, the reaction mixture was refrigerated overnight. A plaster-like product precipitated. The product was filtered off and washed

thoroughly with cold toluene (10 mL), 2-PrOH (2.5 mL) and distilled H_2O (5 mL). The product was dried in a desiccator with P_2O_5. Raw product (207 mg, 63%) was crystallized from ethanol. White powder. M.p.: 283–286 °C (sublimation preceded melting; product melted at coincident decomposition). HPLC R_t = 16.7 min (80% MeOH + 20% buffer); UV (80% MeOH + 20% buffer) λ_{min} 238 nm, λ_{max} 280 nm. HPLC purity > 98%. MS ESI+ (CV 18) *m/z* (rel. %): 328 $[M+H]^+$ (100), 330 $[M+H]^+$ (48), 350 $[M+Na]^+$ (97), 352 $[M+Na]^+$ (46); ESI$^-$ (CV 19) *m/z* (rel. %): 326 $[M]^-$ (100), 328 $[M]^-$ (42). ^{1}H NMR (500 MHz, DMSO-d_6) δ (ppm): 2.10–2.12 (m, 4H), 3.34 (s, 4H), 4.26 (bs, 4H), 8.12 (s, 1H), 13.18 (bs, 1H). ^{13}C NMR (125 MHz, DMSO-d_6) δ (ppm): 37.9, 41.2, 44.8 (bs), 66.2, 117.7, 138.8, 152.3, 152.6, 153.0.

*4.1.38. 2-(2-Hydroxyethylamino)-6-(1,4-dithia-8-azaspiro[4.5]decan-8-yl)purine (**38**)*

2-Chloro-6-(1,4-dithia-8-azaspiro[4.5]decan-8-yl)purine (**37**; 137 mg, 0.42 mmol) was dissolved in ethanolamine (1.3 mL). The solution was heated at 149 °C for 19 h. After cooling, the product was precipitated with distilled H_2O (10 mL). The suspension was refrigerated overnight. The milk-like precipitate was filtered off, washed thoroughly with distilled H_2O (10 mL), and dried in a desiccator with P_2O_5. Raw product (134 mg, 91%) was crystallized from ethanol. White plaster-like solid. M.p.: 222–224 °C. HPLC R_t = 6.3 min (80% MeOH + 20% buffer), R_t = 8.5 min (70% MeOH + 30% buffer); UV (80% MeOH + 20% buffer) λ_{max} 239 nm, λ_{min} 272 nm, λ_{max} 294 nm. MS ESI+ (CV 18) *m/z* (rel. %): 353 $[M+H]^+$ (100), 375 $[M+Na]^+$ (15); ESI$^-$ (CV 21) *m/z* (rel. %): 351 $[M]^-$ (100). ^{1}H NMR (500 MHz, DMSO-d_6) δ (ppm): 2.04–2.06 (m, 4H), 3.28 (q, J = 6.1 Hz, 2H), 3.33 (s, 4H), 3.43 (qd, J = 7.0, 2.2 Hz, 1H), 3.48–3.51 (m, 2H), 4.20 (bs, 4H), 4.33 (bs, 1H), 6.11 (t, J = 5.8 Hz, 1H), 7.67 (s, 1H), 12.28 (bs, 1H). ^{13}C NMR (125 MHz, DMSO-d_6) δ (ppm): 37.8, 41.4, 43.8, 44.4, 60.2, 66.7, 113.3, 134.7, 153.1, 153.7, 158.7.

*4.1.39. 6-(1,5-Dioxa-9-azaspiro[5.5]undecan-9-yl)purine (**39**)*

1-(Purin-6-yl)piperidin-4-one (**26**; 100 mg, 0.46 mmol) was mixed with toluene (5 mL), 1,3-propanediol (82 µL, 1.13 mmol), and *p*-toluenesulfonic acid monohydrate (93 mg, 0.49 mmol). The mixture was heated at 104 °C for 12 h. Dehydration was ensured by continuous azeotropic distillation. The reaction produced a mixture of a yellowish liquid and a dark brown asphaltic substance on the bottom of the flask. The reaction mixture was mixed with $CHCl_3$ (30 mL) to dissolve solid particles, then shaken with 0.25% Na_2CO_3 (10 mL). The organic layer was dried with Na_2SO_4 and evaporated. The residuum was dissolved in MeOH, adsorbed on silica gel (0.94 g), and purified by column chromatography (gradient chromatography: starting with mobile phase $CHCl_3$, ending with mobile phase $CHCl_3$:MeOH 98:2, flow rate 10 mL/min). White crystals. Yield: 98 mg (77%). M.p.: 272–273 °C (> 220 °C sublimation). HPLC R_t = 8.4 min (60% MeOH + 40% buffer); UV (70% MeOH + 30% buffer) λ_{min} 234 nm, λ_{max} 278 nm. HPLC purity 98%. MS ESI+ (CV 19) *m/z* (rel. %): 276 $[M+H]^+$ (100), 298 $[M+Na]^+$ (17); ESI$^-$ (CV 19) *m/z* (rel. %): 274 $[M]^-$ (100). ^{1}H NMR (300 MHz, $CDCl_3$) δ (ppm): 1.78 (pent., J = 5.6 Hz, 2H, dioxane H5′), 2.01–2.05 (m, 4H, piperidine H3′, H5′), 3.97 (t, J = 5.6 Hz, 4H, dioxane H4′, H6′), 4.37 (bs, 4H, piperidine H2′, H6′), 7.97 (s, 1H, pur H8), 8.38 (s, 1H, pur H2). ^{13}C NMR (75 MHz, $CDCl_3$) δ (ppm): 25.5 (dioxane C5′), 33.1 (piperidine C3′, C5′), 41.8 (bs, piperidine C2′, C6′), 59.4 (dioxane C4′, C6′), 96.3 (spiro C), 119.6 (pur C5), 136.7 (pur C8), 151.1 (pur C4), 151.3 (pur C2), 153.8 (pur C6).

*4.1.40. 6-(3-Hydroxy-1,5-dioxa-9-azaspiro[5.5]undecan-9-yl)purine (**40**)*

1-(Purin-6-yl)piperidin-4-one (**26**; 0.81 g, 3.73 mmol) was mixed with toluene (30 mL), glycerol (0.35 mL, 4.75 mmol) and *p*-toluenesulfonic acid monohydrate (0.71 g, 3.70 mmol). The mixture was heated at 104 °C for 5.5 h. Dehydration was ensured by continuous azeotropic distillation. The reaction produced a mixture of a yellowish liquid and a dark brown asphaltic substance on the bottom of the flask. The reaction mixture was evaporated, and the residuum was dried in a desiccator. The residuum was dissolved in $CHCl_3$:MeOH 2:1 (15 mL) and filtered, and the filtrate was adsorbed on silica gel (2.48 g) and purified by column chromatography (mobile phase $CHCl_3$:MeOH:NH_4OH 95:5:0.5, flow rate 9.3 mL/min). Yellow crystals. Yield: 259 mg (24%). M.p.: 244–245 °C (> 200 °C sublimation; crystallized from $CHCl_3$:MeOH). HPLC R_t = 9.3 min (45% MeOH + 55% buffer); UV (45% MeOH + 55% buffer) λ_{min} 235 nm, λ_{max} 277 nm. HPLC purity > 99%. MS ESI+ (CV 19) *m/z* (rel. %): 292 $[M+H]^+$ (100), 314 $[M+Na]^+$ (27); ESI$^-$ (CV 18) *m/z* (rel. %): 290 $[M]^-$ (100). ^{1}H NMR (500 MHz, DMSO-d_6) δ (ppm): 1.68–1.70 (m, 4H, piperidine H3′, H5′), 3.41 (dd, J = 11.3, 5.8 Hz, 1H, dioxane H4′), 3.46 (dd, J = 11.1, 5.1 Hz, 1H, dioxane H4′), 3.72 (dd, J = 8.4, 6.1 Hz, 1H, dioxane H6′), 4.03 (dd, J = 8.2, 6.4 Hz, 1H, dioxane H6′), 4.10 (dt, J = 11.6, 6.0 Hz, 1H, dioxane H5′), 4.15 (bs overlapped, 2H, piperidine H2′, H6′), 4.36 (bs, 2H, piperidine H2′, H6′), 4.86 (bs, 1H, -OH), 8.10 (s, 1H, pur H8), 8.18 (s, 1H, pur H2), 13.00 (bs, 1H, pur NH). ^{13}C NMR (125 MHz, DMSO-d_6) δ (ppm): 34.6 (piperidine C3′), 35.8 (piperidine C5′), 42.7 (piperidine C2′, C6′), 62.0 (dioxane C6′), 65.9 (dioxane C4′), 76.2 (dioxane C5′-OH), 107.1 (spiro C), 118.8 (pur C5), 138.1 (pur C8), 151.4 (pur C4), 151.8 (pur C2), 152.9 (pur C6).

*4.1.41. 6-(7,12-Dioxa-3-azaspiro[5.6]dodecan-3-yl)purine (**41**)*

1-(Purin-6-yl)piperidin-4-one (**26**; 204 mg, 0.94 mmol) was mixed with toluene (10 mL), 1,4-butandiol (125 µL, 1.41 mmol), and *p*-toluenesulfonic acid monohydrate (176 mg, 0.93 mmol). The mixture was heated at 104 °C for 5.5 h. Dehydration was ensured by continuous azeotropic distillation. The reaction produced a mixture of a yellowish liquid and a dark brown asphaltic substance on the bottom of the flask. The reaction mixture was mixed with $CHCl_3$ (30 mL) to dissolve solid particles, then shaken with 0.25% Na_2CO_3 (16 mL). The product from the water layer was reextracted with $CHCl_3$ (10 mL). The united organic layers were dried with Na_2SO_4 and evaporated. The residuum was dissolved in MeOH, adsorbed on silica gel (1.24 g), and purified by column chromatography (gradient chromatography: starting with mobile phase $CHCl_3$, ending with mobile phase $CHCl_3$:MeOH 96.5:3.5, flow rate 10 mL/min). White plaster-like powder. Yield: 174 mg (64%). M.p.: 250–257 °C. HPLC R_t = 10.7 min (70% MeOH + 30% buffer); UV (70% MeOH + 30% buffer) λ_{min} 234 nm, λ_{max} 277 nm. HPLC purity 98%. MS ESI+ (CV 18) *m/z* (rel. %): 290 $[M+H]^+$ (100), 312 $[M+Na]^+$ (10); ESI$^-$ (CV 19) *m/z* (rel. %): 288 $[M]^-$ (100). ^{1}H NMR (300 MHz, DMSO-d_6) δ (ppm): 1.53 (s, 4H, dioxepane H5′, H6′), 1.69 (s, 4H, piperidine H3′, H5′), 3.65 (s, 4H, dioxepane H4′, H7′), 4.20 (bs, 4H, piperidine H2′, H6′), 8.09 (s, 1H, pur H8), 8.18 (s, 1H, pur H2), 13.01 (bs, 1H, pur NH). ^{13}C NMR (75 MHz, DMSO-d_6) δ (ppm): 29.2 (dioxepane C5′, C6′), 33.6 (piperidine C3′, C5′), 42.0 (bs, piperidine C2′, C6′), 61.1 (dioxepane C4′, C7′), 99.1 (spiro C), 118.8 (pur C5), 137.9 (pur C8), 151.3 (pur C4), 151.7 (pur C2), 152.9 (pur C6).

*4.1.42. 6-(Azepan-1-yl)-3-methylpurine (**42**)*

6-(Azepan-1-yl)purine (0.15 g, 0.65 mmol) was heated with MeI (0.146 mL, 2.35 mmol) in DMA (4.6 mL) at 80 °C until complete consumption of starting material, monitored by TLC ($CHCl_3$:MeOH 9:1). Then, the reaction mixture was diluted with saturated $NaHCO_3$ (10 mL) and extracted by EtOAc (5 × 10 mL). Combined organic layers were washed with water (5 mL), brine (15 mL), dried over Na_2SO_4 and evaporated *in vacuo*. Crude product was purified by silica column chromatography using $CHCl_3$:MeOH as a mobile phase with MeOH gradient. Yield: 28 mg (19%). HPLC purity > 97%. MS ESI+ (CV 20) *m/z* (rel. %): 232 $[M+H]^+$ (100). ^{1}H NMR (500 MHz, DMSO-d_6) δ (ppm): 1.48 (bs, 4H, azep H4′, 5′), 1.75–1.81 (m, 4H, azep H3′, 6′), 3.86–3.89 (m, 5H, azep H2′, -CH_3), 4.47 (t, J = 6.0 Hz, 2H, azep H7′), 7.73 (s, 1H, pur H8), 8.32 (s, 1H, pur H2). ^{13}C NMR (125 MHz, DMSO-d_6) δ (ppm): 25.9 (azep C4′), 26.3 (azep C5′), 26.7 (azep C3′), 28.4 (azep C6′), 35.7 (CH_3), 48.3 (azep C2′), 49.3 (azep C7′), 120.4 (pur C5), 142.9 (pur C2), 150.5 (pur C4), 151.7 (pur C8), 152.2 (pur C6).

*4.1.43. 6-(Pyrrolidin-1-yl)purine (**44**)*

A suspension of 6-chloropurine (150 mg, 0.97 mmol), pyrrolidine (97 μL, 1.17 mmol) and Et_3N (338 μL, 2.43 mmol) in *n*-PrOH (3.83 mL) was heated in MW reactor Discover SP (CEM Corporation) at 120 °C for 10 min. Reaction mixture was cooled at 4 °C for 30 min and resulting white solid was filtered, washed with ice cold *n*-PrOH (3 × 1 mL), water (3 × 1 mL) and dried at 50 °C. Crude material was purified by silica column chromatography using $CHCl_3$:MeOH as a mobile phase with MeOH gradient. Yield: 159 mg (87%). HPLC purity > 99%. ESI + (CV 20) *m/z* (rel. %): 190 $[M+H]^+$ (100). ^{1}H NMR (500 MHz, DMSO-d_6) δ (ppm): 1.94 (bs, 4H, pyr H3, pyr H3′, pyr H4, pyr H4′), 3.62 (bs, 2H, pyr H2, pyr H2′), 4.07 (bs, 2H, pyr H5, pyr H5′), 8.04 (s, 1H, pur H8), 8.15 (s, 1H, pur H2), 12.87 (bs, 1H, pur H7/9). ^{13}C NMR (125 MHz, DMSO-d_6) δ (ppm): 23.8 (pyr C3), 25.7 (pyr C4), 46.8 (pyr C2), 48.4 (pyr C5), 119.1 (pur C5), 138.1 (pur C8), 150.6 (pur C4), 152.1 (pur C2), 152.4 (pur C6).

*4.1.44. 2-Chloro-6-(pyrrolidin-1-yl)purine (**45**)*

A suspension of 2,6-dichloropurine (0.5 g, 2.65 mmol), pyrrolidine (265 μL, 3.18 mmol), Et_3N (920 μL, 6.61 mmol) in *n*-PrOH (17.6 mL) was heated at 90 °C for 3 h. Solvents were evaporated under reduced pressure and the residue was treated with water (15 mL). Resulting white solid was filtered, washed with water (3 × 2 mL) and dried at 50 °C. The pure compound was obtained after recrystallization from MeOH. Yield: 563 mg (95%). M.p.: > 300 °C. HPLC purity > 99%. ESI + (CV 20) *m/z* (rel. %): 224 $[^{35}Cl\text{-}M+H]^+$ (100), 226 $[^{37}Cl-M+H]^+$ (34). ^{1}H NMR (500 MHz, DMSO-d_6) δ (ppm): 1.87–1.90 (m, 2H, pyr H3, pyr H3′), 1.96–1.99 (m, 2H, pyr H4, pyr H4′), 3.56 (bs, 2H, pyr H2, pyr H2′), 4.04 (bs, 2H, pyr H5, pyr H5′), 8.07 (s, 1H, pur H8), 13.06 (bs, 1H, pur H7/9). ^{13}C NMR (125 MHz, DMSO-d_6) δ (ppm): 23.6 (pyr C3), 25.6 (pyr C4), 47.1 (pyr C2), 48.6 (pyr C5), 118.1 (pur C5), 138.8 (pur C8), 151.6 (pur C4), 152.6 (pur C6), 152.7 (pur C2).

*4.1.45. 2-(2-Hydroxyethylamino)-6-(pyrrolidin-1-yl)purine (**46**)*

2-chloro-6-(pyrrolidin-1-yl)purine (**45**) (150 mg, 0.67 mmol) was heated with ethanolamine (607 μL, 10.06 mmol) at 165 °C for 3 h. Reaction mixture was diluted with water (10 mL), cooled at 4 °C for 1 h and resulting white solid was filtered, washed with ice cold water (3 × 1 mL) and dried at 50 °C. The pure compound was obtained after recrystallization from EtOH. Yield: 130 mg (78%). M.p.: 245–247 °C. HPLC purity > 99%. ESI + (CV 20) *m/z* (rel. %): 249 $[M+H]^+$ (100). ^{1}H NMR (500 MHz, DMSO-d_6) δ (ppm): ^{1}H NMR (500 MHz, DMSO-d_6) δ (ppm): 1.89 (bs, 4H, pyr H3, pyr H3′, pyr H4, pyr H4′), 3.29 (q, J = 6.0 Hz, 2H, $NHC\underline{H}_2CH_2OH$), 3.50 (q, J = 5.5 Hz, 2H, $NHCH_2C\underline{H}_2OH$), 3.55 (bs, 2H), 3.96 (bs, 2H), 4.70 (t, J = 4.8 Hz, 1H, $NHCH_2CH_2O\underline{H}$), 6.00 (t, J = 5.7 Hz, 1H, $N\underline{H}CH_2CH_2OH$), 7.61 (s, 1H, pur H8), 12.13 (bs, 1H, pur 7/9). ^{13}C NMR (125 MHz, DMSO-d_6) δ (ppm): 23.8 (pyr C3), 25.6 (pyr C4), 43.9 ($NHC\underline{H}_2CH_2OH$), 46.5 (pyr C2), 47.9 (pyr C5), 60.5 ($NHCH_2C\underline{H}_2OH$), 113.7 (pur C5), 134.7 (pur C8), 152.7 (pur C4), 152.8 (pur C6), 159.1 (pur C2).

*4.1.46. 2-(3-Hydroxypropylamino)-6-(pyrrolidin-1-yl)purine (**47**)*

2-chloro-6-(pyrrolidin-1-yl)purine (**45**) (150 mg, 0.67 mmol) was heated with 3-aminopropanol (769 μL, 10.06 mmol) at 165 °C for 3 h. Reaction mixture was diluted with water (10 mL), cooled at 4 °C for 1 h and resulting white solid was filtered, washed with ice cold water (3 × 1 mL) and dried at 50 °C. The pure compound was obtained after recrystallization from MeOH. Yield: 140 mg (80%). M.p.: 224–225 °C. HPLC purity > 99%. ESI + (CV 20) *m/z* (rel. %): 263 $[M+H]^+$ (100). ^{1}H NMR (500 MHz, DMSO-d_6) δ (ppm): 1.64 (pent., J = 6.4 Hz, 2H, $NHCH_2C\underline{H}_2CH_2OH$), 1.88 (bs, 4H, pyr H3, pyr H3′, pyr H4, pyr H4′), 3.27 (q, J = 6.5 Hz, 2H, $NHC\underline{H}_2CH_2CH_2OH$), 3.44 (q, J = 6.0 Hz, 2H, $NHCH_2CH_2C\underline{H}_2OH$), 3.56 (bs, 2H, pyr C2), 3.95 (bs, 2H, pyr C5), 4.49 (t, J = 5.0 Hz, 1H, $NHCH_2CH_2CH_2O\underline{H}$), 6.10 (t, J = 5.8 Hz, 1H, $N\underline{H}CH_2CH_2CH_2OH$), 7.60 (s, 1H, pur H8), 12.15 (bs, 1H, pur H7/9). ^{13}C NMR (125 MHz, DMSO-d_6) δ (ppm): 24.0 (pyr C3), 25.6 (pyr C4), 32.7 ($NHCH_2\underline{C}H_2CH_2OH$), 38.2 ($NH\underline{C}H_2CH_2CH_2OH$), 46.6 (pyr C2), 47.9 (pyr C5), 58.8 ($NHCH_2CH_2\underline{C}H_2OH$), 113.5 (pur C5), 134.6 (pur C8), 152.8 (pur C4), 152.9 (pur C6), 159.2 (pur C2).

4.2. Cell culture and reagents

The A375m2 melanoma cell line was kindly provided by Professor R. Hynes, while the A2058 (melanoma), HT1080 (fibrosarcoma), BJ (skin fibroblasts), and ARPE-19 (retinal epithelium cells) were purchased from ATCC. The keratinocytes HaCaT were from CLS. All cell lines were cultured in Dulbecco's Modified Eagle Medium (Sigma, D6429) supplemented with 10% fetal bovine serum (Sigma, F7524), at 37 °C and 5% CO_2. Rat collagen was purchased from Serva (Cat. No. 4256.01), and the following antibodies were used: MLC2 antibody (Cell Signaling, 3672), pMLC2 (T18/S19) (Cell Signaling, 3674P), rabbit anti mouse (Abcam, ab97046), and goat anti-rabbit (Santa Cruz Biotechnology, sc-2030). Recombinant ROCK2 kinase and its peptide substrate were from Proquinase. Fasudil and Y-28632 ROCK inhibitors were purchased from Santa Cruz Biotechnology (sc-2034 and sc-3536, respectively).

4.3. In vitro kinase assay

ROCK2 kinase was purchased from ProQinase GmbH. Kinase-inhibitory activity of each test compound was assayed using a mixture of the following in a final volume of 10 μL: 0.1 mg/mL tetra (LRRWSLG), 5 μM ATP; 0.05 μCi [γ-^{33}P]ATP; the test compound; and reaction buffer. The reaction buffer consisted of 60 mM HEPES-NaOH, pH 7.5, 3 mM $MgCl_2$, 3 mM $MnCl_2$, 3 μM Na-orthovanadate, 1.2 mM DTT, and 50 μg/mL $PEG_{20.000}$. The reactions were stopped by adding 5 μL of 3% aqueous H_3PO_4. Aliquots were spotted onto P-81 phosphocellulose (Whatman), washed 3 times with 0.5% aqueous H_3PO_4, and finally air-dried. Kinase inhibition was quantified using a FLA-7000 digital image analyzer (Fujifilm). The concentrations required to decrease ROCK2 activity by 50% (IC_{50}) were calculated from the dose-response curves.

4.4. In vitro evaluation of anti-proliferative activity

In vitro toxicity of the compounds for BJ, HaCaT, ARPE-19, A375m2, A2058, and HT1080 cells was evaluated using the resazurin reduction assay. Resazurin is a blue weakly-fluorescent compound that is irreversibly reduced into red highly-fluorescent resofurin by metabolically-active cells. The effects of the test compounds at 6 concentrations (maximum concentration of 100 μM and 5 two-fold dilutions) were evaluated after a 72-h treatment. DMSO vehiculum served as a negative control. The cells were maintained under standard cultivation conditions (5.5% CO_2, 37 °C, 100% humidity). The cultivation medium was DMEM with 10% FBS. For the cytotoxicity evaluation, the cells were trypsinized and pipetted into 96-well plates (5000 cells per well in 80 μL). After 24 h, 5× concentrated solutions of the test compounds were added to the medium. After 72 h, a 10× concentrated solution of resazurin in medium (prepared from 1000× concentrated DMSO solution) was added to the cells on the plate for final concentration of 100 μM per well. Fluorescence (ex = 570 nm, em = 610 nm) was measured after 1 h (ARPE-19) or 3 h (HaCaT and BJ) of incubation. IC_{50} values were calculated from dose-response curves using the drc library for the R programming environment.

4.5. 3D morphology assay

Cells at a population of 10^4-1.5x10^4 cells (about 10% of the total collagen volume) were seeded into 250 μL, 1.5 mg/mL rat collagen (18% 5× DMEM, 23.26% H_2O, 5% of 7.5% $NaHCO_3$, 4.24% of 200 mM NaOH, 2% of 750 mM Hepes, 37.5% of 4% rat collagen) in a 48-well tissue culture plate (Biofil, 011048), in the presence of 10 μM ROCK inhibitors, or DMSO as a control. After solidification, 500 μL of culture

media with 10 μM ROCK inhibitors was added on top of the collagen. Morphological changes were evaluated after 24 h, and cells with length twice as long as their width were considered mesenchymal. Experiments were repeated at least 3 times.

4.6. Invasion assay

The invasion assay was performed in Ibidi 15μ-Slide Angiogenesis plates (ibidi, 81506) in 10 μL 1 mg/mL rat collagen (composition similar to the 3D morphology assay described above) containing 10 μM ROCK inhibitors, or DMSO as a control. Cells at a population of 10^3 were seeded on top of collagen in 50 μL of culture media with inhibitors. This media was changed to serum-free media with inhibitors after 6–8 h. Cells were imaged 72 h after being seeded, with images taken at 10-μm depth intervals in the collagen using a Nikon-Eclipse TE2000-S (20×/0.40 HMC objective) and NIS-Elements software. For each experiment, invasion was analysed in 3 wells, and average invasion depth was assessed in 6 fields of view per individual well. The average invasion depth was normalized to that of untreated cells to compare individual experiments. Three independent experiments were analysed for each condition. Statistical analysis using the R programming environment involved ANOVA followed by Tukey's honest significant difference test.

4.7. Western-blotting

Cells were lysed with cold lysis buffer containing: 1% Triton X-100 in Tris-buffered saline (25 mM Tris, 150 mM sodium chloride, pH 7.4), protease inhibitors mixB (Serva, 20384.07), and phosphatase inhibitors mixII (Serva, 39055.01). Cell lysates were resolved on 10% SDS-PAGE, and proteins were transferred electrophoretically to Amersham™ Proton™ 0.45 μm nitrocellulose blotting membranes. Nonspecific activity was blocked by incubating membranes for 1 h at room temperature in Tris-buffered saline containing 4% bovine serum albumin (BSA; Sigma, A7030) and 1% non-fat dry milk. Membranes were then incubated overnight at 4 °C with primary antibodies (in 1% BSA in Tris-buffered saline 0.1% Tween20 (TTBS)), washed extensively with TTBS, and incubated for 1 h at room temperature with horseradish peroxidase (HRP)-conjugated secondary antibodies. After extensive washing in TTBS, the blots were developed using SuperSignal West Pico Chemiluminescent substrate (Thermo Scienfic 34080) on a LAS-1000 Single System (Fujifilm, Tokyo, Japan). Densitometric quantification of Western blots was carried out using ImageJ software (http://rsbweb.nih.gov/ij/).

Acknowledgement

We are grateful to Kateřina Faksová and Jana Hudcová for their superb technical assistance and to Martin Hönig for recording of NMR spectra. This work was also supported by the Ministry of Education, Youth and Sports, Czech Republic (Grants LO1204 and LO1304 from the National Program of Sustainability I, the project BIOCEV-FAR (Reg. No. LQ1604) from National Program of Sustainability II, the project BIOCEV (CZ.1.05/1.1.00/02.0109)), by the Czech Grant Agency (Grant Nos. 17-14007S and 15-17419S) and by Palacky University (IGA_PrF_2018_006).

Appendix A. Supplementary material

Supplementary data to this article can be found online at https://doi.org/10.1016/j.bioorg.2019.103005.

References

[1] H. Aizawa, S. Wakatsuki, A. Ishii, K. Moriyama, Y. Sasaki, K. Ohashi, Y. Sekine-Aizawa, A. Sehara-Fujisawa, K. Mizuno, Y. Goshima, I. Yahara, Phosphorylation of cofilin by LIM-kinase is necessary for semaphorin 3A-induced growth cone collapse, Nat. Neurosci. 4 (2001) 367–373, https://doi.org/10.1038/86011.

[2] C.E. Allen, C.L. Chow, J.J. Caldwell, I.M. Westwood, R.L.M. van Montfort, I. Collins, Synthesis and evaluation of heteroaryl substituted diazaspirocycles as scaffolds to probe the ATP-binding site of protein kinases, Bioorg. Med. Chem. 21 (2013) 5707–5724, https://doi.org/10.1016/j.bmc.2013.07.021.

[3] S.R. Breshears, S.S. Wang, S.G. Bechtolt, B.E. Christensen, Purines. VIII. The Aminolysis of Certain Chlorosubstituted Purines, J. Am. Chem. Soc. 81 (1959) 3789–3792, https://doi.org/10.1021/ja01523a075.

[4] K.W. Cheng, R. Agarwal, G.B. Mills, Ras-superfamily GTP-ases in ovarian cancer, Cancer Treat. Res. 149 (2009) 229–240, https://doi.org/10.1007/978-0-387-98094-2_11.

[5] O. Defert, S. Boland, Rho kinase inhibitors: a patent review (2014–2016), Expert Opin. Ther. Pat. 27 (2017) 507–515, https://doi.org/10.1080/13543776.2017.1272579.

[6] C. Dyberg, S. Fransson, T. Andonova, B. Sveinbjörnsson, J. Lännerholm-Palm, T.K. Olsen, D. Forsberg, E. Herlenius, T. Martinsson, B. Brodin, P. Kogner, J.I. Johnsen, M. Wickström, Rho-associated kinase is a therapeutic target in neuroblastoma, Proc. Natl. Acad. Sci. 114 (2017) E6603–E6612, https://doi.org/10.1073/pnas.1706011114.

[7] Y. Feng, P.V. LoGrasso, O. Defert, R. Li, Rho Kinase (ROCK) inhibitors and their therapeutic potential, J. Med. Chem. 59 (2016) 2269–2300, https://doi.org/10.1021/acs.jmedchem.5b00683.

[8] Y. Feng, P.V. LoGrasso, Rho kinase inhibitors: a patent review (2012–2013), Expert Opin. Ther. Pat. 24 (2014) 295–307, https://doi.org/10.1517/13543776.2014.863279.

[9] G. Gadea, V. Sanz-Moreno, A. Self, A. Godi, C.J. Marshall, DOCK10-mediated Cdc42 activation is necessary for amoeboid invasion of melanoma cells, Curr. Biol. 18 (2008) 1456–1465, https://doi.org/10.1016/j.cub.2008.08.053.

[10] C. Greenman, P. Stephens, R. Smith, G.L. Dalgliesh, C. Hunter, G. Bignell, H. Davies, J. Teague, A. Butler, C. Stevens, S. Edkins, S. O'Meara, I. Vastrik, E.E. Schmidt, T. Avis, S. Barthorpe, G. Bhamra, G. Buck, B. Choudhury, J. Clements, J. Cole, E. Dicks, S. Forbes, K. Gray, K. Halliday, R. Harrison, K. Hills, J. Hinton, A. Jenkinson, D. Jones, A. Menzies, T. Mironenko, J. Perry, K. Raine, D. Richardson, R. Shepherd, A. Small, C. Tofts, J. Varian, T. Webb, S. West, S. Widaa, A. Yates, D.P. Cahill, D.N. Louis, P. Goldstraw, A.G. Nicholson, F. Brasseur, L. Looijenga, B.L. Weber, Y.-E. Chiew, A. deFazio, M.F. Greaves, A.R. Green, P. Campbell, E. Birney, D.F. Easton, G. Chenevix-Trench, M.-H. Tan, S.K. Khoo, B.T. Teh, S.T. Yuen, S.Y. Leung, R. Wooster, P.A. Futreal, M.R. Stratton, Patterns of somatic mutation in human cancer genomes, Nature 446 (2007) 153–158, https://doi.org/10.1038/nature05610.

[11] F. Grise, A. Bidaud, V. Moreau, Rho GTPases in hepatocellular carcinoma, BBA 1795 (2009) 137–151, https://doi.org/10.1016/j.bbcan.2008.12.003.

[12] G. Huet, K.-P. Skarp, M.K. Vartiainen, Nuclear actin levels as an important transcriptional switch, Transcription 3 (2012) 226–230, https://doi.org/10.4161/trns.21062.

[13] M. Iizuka, K. Kimura, S. Wang, K. Kato, M. Amano, K. Kaibuchi, A. Mizoguchi, Distinct distribution and localization of Rho-kinase in mouse epithelial, muscle and neural tissues, Cell Struct. Funct. 37 (2012) 155–175.

[14] K. Itoh, K. Yoshioka, H. Akedo, M. Uehata, T. Ishizaki, S. Narumiya, An essential part for Rho-associated kinase in the transcellular invasion of tumor cells, Nat. Med. 5 (1999) 221–225, https://doi.org/10.1038/5587.

[15] P.Y. Jay, P.A. Pham, S.A. Wong, E.L. Elson, A mechanical function of myosin II in cell motility, J. Cell Sci. 108 (Pt 1) (1995) 387–393.

[16] P. Kocieński, Chapter 2 Carbonyl protecting groups, Protecting Groups, 3rd edition Georg Thieme Verlag, Stuttgart, New York, ISBN 3-13-135603-0 (GTV), ISBN 1-58890-376-1 (TNY), 2005.

[17] J. Kosla, D. Paňková, J. Plachý, O. Tolde, K. Bicanová, M. Dvořák, D. Rösel, J. Brábek, Metastasis of aggressive amoeboid sarcoma cells is dependent on Rho/ROCK/MLC signaling, Cell Commun. Signal. 30 (11) (2013 Jul) 51, https://doi.org/10.1186/1478-811X-11-51 PubMed PMID: 23899007.

[18] J. Lane, T.A. Martin, G. Watkins, R.E. Mansel, W.G. Jiang, The expression and prognostic value of ROCK I and ROCK II and their role in human breast cancer, Int. J. Oncol. 33 (2008) 585–593.

[19] D.A. Lauffenburger, A.F. Horwitz, Cell migration: a physically integrated molecular process, Cell 84 (1996) 359–369.

[20] K. Liu, X. Li, J. Wang, Y. Wang, H. Dong, J. Li, Genetic variants in RhoA and ROCK1 genes are associated with the development, progression and prognosis of prostate cancer, Oncotarget 8 (2017) 19298–19309, https://doi.org/10.18632/oncotarget.15197.

[21] X. Liu, E. Choy, F.J. Hornicek, S. Yang, C. Yang, D. Harmon, H. Mankin, Z. Duan, ROCK1 as a potential therapeutic target in osteosarcoma, J. Orthop. Res. 29 (2011) 1259–1266, https://doi.org/10.1002/jor.21403.

[22] P.A. Lochhead, G. Wickman, M. Mezna, M.F. Olson, Activating ROCK1 somatic mutations in human cancer, Oncogene 29 (2010) 2591–2598, https://doi.org/10.1038/onc.2010.3.

[23] G. Loirand, Rho kinases in health and disease: from basic science to translational research, Pharmacol. Rev. 67 (2015) 1074–1095, https://doi.org/10.1124/pr.115.010595.

[24] T. Matsuoka, M. Yashiro, Rho/ROCK signaling in motility and metastasis of gastric cancer, World J. Gastroenterol. 20 (2014) 13756–13766, https://doi.org/10.3748/wjg.v20.i38.13756.

[25] S. Micuda, D. Rösel, A. Ryska, J. Brábek, ROCK inhibitors as emerging therapeutic candidates for sarcomas, Curr. Cancer Drug Targets 10 (2010) 127–134.

[26] J. Montgomery, L. Holum, Synthesis of Potential Anticancer Agents. III. Hydrazino Analogs of Biologically Active Purines 2 (1957).

[27] M. Morgan-Fisher, U.M. Wewer, A. Yoneda, Regulation of ROCK activity in cancer, J. Histochem. Cytochem. 61 (2013) 185–198, https://doi.org/10.1369/0022155412470834.
[28] M. Nakajima, K. Hayashi, K. Katayama, Y. Amano, Y. Egi, M. Uehata, N. Goto, T. Kondo, Wf-536 prevents tumor metastasis by inhibiting both tumor motility and angiogenic actions, Eur. J. Pharmacol. 459 (2003) 113–120.
[29] J.M.J. Nolsøe, L.-L. Gundersen, F. Rise, Synthesis of 8-halopurines by reaction of lithiated purines with appropriate halogen donors, Synth. Commun. 28 (1998) 4303–4315.
[30] K. Noma, N. Oyama, J.K. Liao, Physiological role of ROCKs in the cardiovascular system, Am. J. Physiol. Cell Physiol. 290 (2006) C661–C668, https://doi.org/10.1152/ajpcell.00459.2005.
[31] K. Panková, D. Rösel, M. Novotný, J. Brábek, The molecular mechanisms of transition between mesenchymal and amoeboid invasiveness in tumor cells, Cell. Mol. Life Sci. 67 (2010) 63–71, https://doi.org/10.1007/s00018-009-0132-1.
[32] D. Paňková, N. Jobe, M. Kratochvílová, R. Buccione, J. Brábek, D. Rösel, NG2-mediated Rho activation promotes amoeboid invasiveness of cancer cells, Eur. J. Cell Biol. 91 (11-12) (2012) 969–977, https://doi.org/10.1016/j.ejcb.2012.05.001 Epub 2012 Jun 13. PubMed PMID: 22699001.
[33] R.A. Patel, K.D. Forinash, R. Pireddu, Y. Sun, N. Sun, M.P. Martin, E. Schonbrunn, N.J. Lawrence, S.M. Sebti, RKI-1447 is a potent inhibitor of the rho-associated ROCK kinases with anti-invasive and antitumor activities in breast cancer, Cancer Res. 72 (2012) 5025–5034, https://doi.org/10.1158/0008-5472.CAN-12-0954.
[34] M. Raftopoulou, A. Hall, Cell migration: Rho GTPases lead the way, Dev. Biol. 265 (2004) 23–32.
[35] A.J. Ridley, Rho GTPases and actin dynamics in membrane protrusions and vesicle trafficking, Trends Cell Biol. 16 (2006) 522–529, https://doi.org/10.1016/j.tcb.2006.08.006.
[36] I. Rodriguez-Hernandez, G. Cantelli, F. Bruce, V. Sanz-Moreno, Rho, ROCK and actomyosin contractility in metastasis as drug targets. F1000Research 5 (2016) 783. doi: 10.12688/f1000research.7909.1.
[37] A. Routhier, M. Astuccio, D. Lahey, N. Monfredo, A. Johnson, W. Callahan, A. Partington, K. Fellows, L. Ouellette, S. Zhidro, C. Goodrow, A. Smith, K. Sullivan, P. Simone, L. Le, B. Vezuli, M. Zohni, E. West, D. Gleason, B. Bryan, Pharmacological inhibition of Rho-kinase signaling with Y-27632 blocks melanoma tumor growth, Oncol. Rep. 23 (2010) 861–867.
[38] A. Sadok, A. McCarthy, J. Caldwell, I. Collins, M.D. Garrett, M. Yeo, S. Hooper, E. Sahai, S. Kuemper, F.K. Mardakheh, C.J. Marshall, Rho kinase inhibitors block melanoma cell migration and inhibit metastasis, Cancer Res. 75 (2015) 2272–2284, https://doi.org/10.1158/0008-5472.CAN-14-2156.
[39] E. Sahai, C.J. Marshall, Differing modes of tumour cell invasion have distinct requirements for Rho/ROCK signalling and extracellular proteolysis, Nat. Cell Biol. 5 (2003) 711–719, https://doi.org/10.1038/ncb1019.
[40] V. Sanz-Moreno, G. Gadea, J. Ahn, H. Paterson, P. Marra, S. Pinner, E. Sahai, C.J. Marshall, Rac activation and inactivation control plasticity of tumor cell movement, Cell 135 (2008) 510–523, https://doi.org/10.1016/j.cell.2008.09.043.
[41] V. Sanz-Moreno, C. Gaggioli, M. Yeo, J. Albrengues, F. Wallberg, A. Viros, S. Hooper, R. Mitter, C.C. Féral, M. Cook, J. Larkin, R. Marais, G. Meneguzzi, E. Sahai, C.J. Marshall, ROCK and JAK1 signaling cooperate to control actomyosin contractility in tumor cells and stroma, Cancer Cell 20 (2011) 229–245, https://doi.org/10.1016/j.ccr.2011.06.018.
[42] S. Shah, J. Savjani, A review on ROCK-II inhibitors: From molecular modelling tosynthesis, Bioorg. Med. Chem. Lett. 26 (10) (2016) 2383–2391.
[43] D. Taddei, P. Kilián, A.M.Z. Slawin, D.J. Woollins, Synthesis and full characterisation of 6-chloro-2-iodopurine, a template for the functionalisation of purines, Org. Biomol. Chem. 2 (2004) 665–670.
[44] M. Takamura, M. Sakamoto, T. Genda, T. Ichida, H. Asakura, S. Hirohashi, Inhibition of intrahepatic metastasis of human hepatocellular carcinoma by Rho-associated protein kinase inhibitor Y-27632, Hepatology 33 (2001) 577–581, https://doi.org/10.1053/jhep.2001.22652.
[45] Y. Tang, L. Olufemi, M.-T. Wang, D. Nie, Role of Rho GTPases in breast cancer, Front. Biosci. 13 (2008) 759–776.
[46] K. Ueda, M. Murata-Hori, M. Tatsuka, H. Hosoya, Rho-kinase contributes to diphosphorylation of myosin II regulatory light chain in nonmuscle cells, Oncogene 21 (2002) 5852–5860, https://doi.org/10.1038/sj.onc.1205747.
[47] C.-L. Wang, O. Lee, G. Hsiao, J.-F. Lian, Y.-W. Cheng, Novel piperazinediones as antitumor agents, Anticancer Res. 34 (2014) 4013–4019.
[48] L. Wei, M. Surma, S. Shi, N. Lambert-Cheatham, J. Shi, Novel insights into the roles of rho kinase in cancer, Arch. Immunol. Ther. Exp. (Warsz) 64 (2016) 259–278, https://doi.org/10.1007/s00005-015-0382-6.
[49] C.C.-L. Wong, C.-M. Wong, E.K.-K. Tung, K. Man, I.O.-L. Ng, Rho-kinase 2 is frequently overexpressed in hepatocellular carcinoma and involved in tumor invasion, Hepatology 49 (2009) 1583–1594, https://doi.org/10.1002/hep.22836.
[50] H. Ying, S.L. Biroc, W.-W. Li, B. Alicke, J.-A. Xuan, R. Pagila, Y. Ohashi, T. Okada, Y. Kamata, H. Dinter, The Rho kinase inhibitor fasudil inhibits tumor progression in human and rat tumor models, Mol. Cancer Ther. 5 (2006) 2158–2164, https://doi.org/10.1158/1535-7163.MCT-05-0440.